Fuel 405 (2026) 136440

Contents lists available at ScienceDirect

Fuel

journal homepage: www.elsevier.com/locate/jfue

Full length article

Generalization of Oberlack's definition of the MILD combustion regime

Adam Klimanek [a,*], Sławomir Sładek [a], Katarzyna Bizon [b], Wojciech Kostowski [a], Michał T. Lewandowski [c], Nils Erland L. Haugen [d,e]

[a] Department of Thermal Technology, Silesian University of Technology, Konarskiego 22, Gliwice, 44-100, Poland
[b] Faculty of Chemical Engineering and Technology, Cracow University of Technology, Warszawska 24, Kraków, 31-155, Poland
[c] Department of Energy and Process Engineering, Norwegian University of Science and Technology, Kolbjørn Hejes vei 1B, Trondheim, NO-7491, Norway
[d] SINTEF Energi A.S., Sem Saelands vei 11, Trondheim, 7034, Norway
[e] Energy Engineering, Div. Energy Science, Luleå University of Technology, Luleå, 971 87, Sweden

HIGHLIGHTS

- Oberlack's definition of the MILD combustion regime has been generalized.
- The previously adopted assumption regarding lean mixture combustion has not been made.
- A new, more general formula for the S-curve (Da vs T) is derived.
- A methodology for finding the boundary of the MILD combustion regime is presented.
- General and fuel-specific (H_2, CH_4) MILD combustion boundaries were determined.

ARTICLE INFO

Keywords:
MILD combustion
MILD regime definition
Homogeneous flow reactor
One-step reaction

ABSTRACT

The Oberlack definition of the MILD combustion limit for premixed systems was derived under the assumption of lean combustion and a one-step reaction. In this study, a generalization of this definition is presented by removing the lean combustion assumption, which leads to a more comprehensive relation between the Damköhler number and temperature, defining the so-called S-curve. The transition of the S-curve to a monotonic function, indicating MILD conditions in the generalized formulation, reveals a dependency on the kinetic parameters of the reaction (reaction orders) and the equivalence ratio. Unlike the previous definition, the proposed solution applies across a broader range of conditions, from rich to lean mixtures, incorporating variations in combustion conditions and the reactivity of the analyzed system. Analytical solutions are not available due to the strong non-linearity of the model; therefore, the results are obtained numerically and are presented as plots and approximation functions, all valid in a wide range of parameter values and applicable to various fuels. The proposed methodology is adaptable to different parameter ranges if needed. Finally, two practical examples, based on hydrogen and methane, illustrate the findings. The results show that reaction orders and the equivalence ratio significantly influence the limit curve defining the MILD combustion regime, with dependencies on the combustion conditions and the chosen fuel.

1. Introduction

Moderate or Intense Low oxygen Dilution (MILD) is a combustion technique that offers high combustion efficiency, low combustion instability, low NO_x and soot emissions [1]. Terms such as Flameless Combustion, Flameless Oxidation, High Temperature Air Combustion, High Temperature Combustion Technology, and Colourless Distributed Combustion refer to the MILD combustion mode or slightly different concepts [1,2]. The advantages of MILD combustion have been noticed in the past and applied in various industries; however, its use is sometimes limited because of its disadvantages, such as high pressure drop, lower operating range, and high volume of reactors/combustors, which sometimes makes integration of this technology difficult.

Several definitions of the MILD combustion regime exist. These include the criteria provided by Oberlack et al. [3], Cavaliere and de Joannon [4], and Evans et al. [5]. The combustion regime boundaries

* Corresponding author.
Email address: adam.klimanek@polsl.pl (A. Klimanek).

https://doi.org/10.1016/j.fuel.2025.136440
Received 13 May 2025; Received in revised form 30 July 2025; Accepted 2 August 2025
Available online 12 August 2025

Nomenclature

Latin symbols

A	Pre-exponential factor, 1/s
c	Molar concentration, kmol/m^3
c_p	Specific heat, J/kgK
Da	Damköhler number
E	Non-dimensional activation energy
E^*	Activation energy, J/kmol
m	Mass, kg
$\dot{m}$	Mass flow rate, kg/s
Q	Non-dimensional heat of combustion
Q^*	Heat of combustion, J/kmol
R	Universal gas constant, J/kmolK
t	Non-dimensional time
t^*	Time, s
T	Non-dimensional temperature
T^*	Temperature, K
T_u	Temperature in unburned state, K
u	Unit conversion factor, $(\mathrm{kmol/m^3})^{(1-\alpha-\beta)}$
V	Volume, m^3
W	Molecular weight, kg/kmol
Y	Non-dimensional mass fraction
Y^*	Mass fraction
Y_{Fu}	Mass fraction of fuel in unburned state
Y_{Ou}	Mass fraction of oxidizer in unburned state

Greek symbols

α	Reaction order w.r.t. fuel
β	Reaction order w.r.t. oxidizer
ν	Stoichiometric coefficient
ρ	Density, kg/m^3
ϕ	Equivalence ratio
$\dot{\omega}$	Reaction rate, kmol/m^{3}s

Abbreviations

MILD	Moderate or intense low oxygen dilution

Subscripts

c	Chemical
D	Diluent
F	Fuel
m	Residence
O	Oxidizer
P	Product
u	Unburned state

including the MILD region for gas turbine applications have also been presented graphically by Rao and Levy [6], and later improved by Perpignan et al. [1]. However, there is no precise and generic definition of MILD combustion that could take into account all the details of this complex process, which are of macroscale and microscale character; see the review by Perpignan et al. [1] for a more detailed discussion. Therefore, the debate on the limits of the MILD combustion mode continues in the literature, and as discussed by Evans et al. [5], different approaches are needed for premixed and non-premixed flames. Temperature-based criteria of Cavaliere and de Joannon [4] were used to create practically useful temperature-oxygen concentration diagrams [7,8] allowing the determination of the conditions for obtaining the desired combustion regime. Similar maps were developed for fuel blends [9]. However, these criteria require the definition of a reference temperature and may fail to accurately capture favorable conditions under elevated pressures. Other limitations of these diagrams have been addressed by Srinivasarao et al. [10], who studied the interaction of the MILD regime with other regimes by examining the effect of ignition delay time during the regime transition. The study revealed a consistent and fuel-type-dependent ignition delay time range at the boundary between MILD and no-combustion regions. Although MILD combustion has been shown to reduce not only thermal NOx but also fuel-bound NOx [11,12], it has been demonstrated that, particularly for ammonia blends, satisfying temperature-based MILD combustion criteria alone is insufficient to achieve low NOx emissions [9]. While temperature-based criteria offer a simple and intuitive way to identify MILD combustion, they introduce arbitrary thresholds and fail to capture kinetic and turbulence effects. In contrast, Oberlack's Damköhler-number-based definition naturally accounts for the transition between combustion regimes by analyzing the fundamental combustion process rather than relying on predefined temperature cutoffs. However, our aim is not to settle the debate on what MILD combustion is or how it should be defined, as multiple approaches may be useful for classifying combustion regimes. Instead, we focus on further exploring and generalizing Oberlack's definition, providing a practically useful solution in the form of an approximated numerical model that is easily accessible to other researchers.

Oberlack et al. [3] proposed a definition of the MILD combustion regime using the equations of the homogeneous flow reactor model, which is valid for premixed systems. The definition is based on the observation that under certain conditions the S-shaped curve (T vs. Da) transforms into a monotonic one, so combustion occurs without an abrupt transition from cold reactants to hot products and extinction can occur by gradual reduction of temperature. In Fig. 1 an S-shaped curve is presented, which was obtained for a single value of non-dimensional heat of combustion Q and various activation energies E, as defined in Oberlack et al. [3]. As can be seen, the curve can have two turning points (two extrema of $Da(T)$) for large E, or become monotonic as E becomes smaller. The point at which the two turning points disappear and form an inflection point is considered to be the boundary of MILD combustion. Many works have confirmed the transformation of the complex S-shaped curve with two distinct characteristics of ignition and extinction into a monotonic curve in the case of premixed and non-premixed combustion with a highly preheated inert or oxidizer [13–16]. Furthermore, analysis of non-premixed counterflow flames indicated that the burning of fuel in hot combustion products as an oxidizer leads to a much lower temperature rise during combustion [16]. These observations were also confirmed in the analysis of a well-stirred reactor by Cavaliere and de Joannon [4], which led to their definition of MILD combustion based on the two indicators: the preheated reactants above the self-ignition temperature and the restricted temperature rise (smaller than self-ignition temperature). This assumption has been criticized, since it would suggest that MILD combustion flames do not exhibit extinction and autoignition in their structures, which have been observed, for example, in the Jet in Hot Coflow experiments [1,5]. The definition of Oberlack et al. [3] was obtained with the assumption of a one-step reaction and lean combustion. The assumption of a single-step model is an important weakness of this approach, since it was shown in numerous studies [17–19] that complex chemical kinetics plays an important role in MILD combustion, which differs significantly from conventional deflagrative-diffusive flames. This is due, among other things, to lower temperatures and significantly different compositions of reactants, which in the case of MILD combustion are diluted with combustion products, such as CO_2 and H_2O. The latter play an active role in chemical reactions and affect the ignition

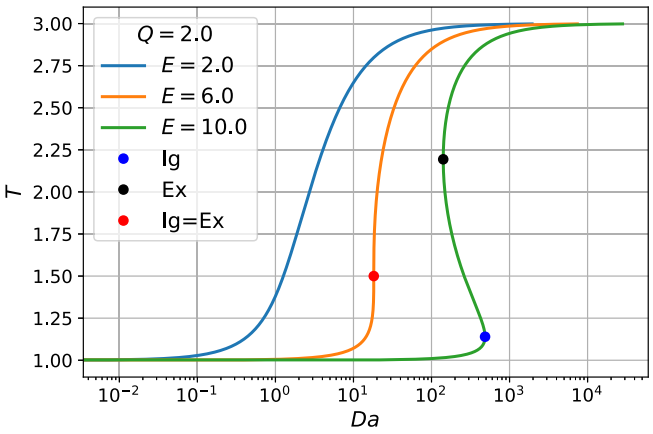

Fig. 1. The S-curves obtained from steady-state solution of the homogeneous flow reactor equations. The MILD regime according to [3] starts when ignition 'Ig' and extinction 'Ex' points meet and the S-curve transforms into a monotonic function; in this case for $E \leq 6.0$.

process, the structure of the reaction zone, the heat release rate, and the overall course of combustion [17,20]. Another weakness is the assumption of lean combustion, which makes this model invalid in rich and near-stoichiometric conditions; however, both assumptions allow for the obtaining of an analytical solution, which in turn enables the examination of important features of the underlying processes.

In this study, we examine the governing equations as presented in Oberlack et al. [3], however, without the assumption of lean combustion. This approach leads to a more complex expression defining the T vs Da curve (the S-curve) than obtained in [3], which now also depends on the inlet fuel and oxidizer concentrations, their reaction orders, and the equivalence ratio. This new expression was then used to identify numerically the conditions at which the boundary of MILD combustion occurs, by employing the definition of Oberlack et al., which is based on the stationary inflection point of the S-curve. Although an analytical solution leading to the criterion of MILD combustion was not found, the numerically determined MILD combustion boundary curves were presented graphically and as approximation functions for various α, β and ϕ, such that one can adapt it to specific one-step reaction characterized by α, β and equivalence ratio. Finally, two examples for CH_4 and H_2 are presented, which show the comparison with the definition of Oberlack et al., and the effect of equivalence ratio on the MILD combustion boundary. In general, the provided solutions can be used to find the unburned/inlet gas temperatures and the corresponding fuel and oxidizer mass fractions, required to obtain the MILD combustion regime.

2. Theory

For a general one-step complete combustion, the reaction can be written as

$$F + \nu O \rightarrow P \tag{1}$$

We assume that the system is composed of fuel F, oxidizer O and diluent D that does not participate in the reaction, and the mass fractions of the species Y_i^* sum to unity

$$Y_F^* + Y_O^* + Y_D^* = 1 \tag{2}$$

Furthermore, we assume that the behavior of the system can be described using a perfectly stirred reactor (PSR) model, which is applicable under near-ideal combustion conditions characterized by infinitely short mixing time, almost perfect mixing of reacting mixture and negligible temperature gradients, resulting in homogeneous composition and temperature throughout the system. Under these assumptions, the rates of change of mass of fuel and oxidizer in a homogeneous flow reactor are

$$m\frac{dY_F^*}{dt^*} = \dot{m}(Y_{Fu} - Y_F^*) + VW_F\dot{\omega}_F \tag{3}$$

$$m\frac{dY_O^*}{dt^*} = \dot{m}(Y_{Ou} - Y_O^*) + VW_O\dot{\omega}_O \tag{4}$$

where Y_{Fu} and Y_{Ou} are the fuel and oxidizer mass fractions in the mixture entering the reactor (the unburned state), W_F and W_O are their molecular weights, V is the reactor volume, and t^* is time. The rates of production/consumption of fuel and the oxidizer are

$$\dot{\omega}_F = -\dot{\omega} \tag{5}$$

$$\dot{\omega}_O = -\nu\dot{\omega} \tag{6}$$

where $\dot{\omega}$ is the reaction rate

$$\dot{\omega} = Au\exp\left(-\frac{E^*}{RT^*}\right)\left(\frac{\rho Y_F^*}{W_F}\right)^{\alpha}\left(\frac{\rho Y_O^*}{W_O}\right)^{\beta} \tag{7}$$

where A is the pre-exponential factor, u is a unit conversion factor $u = 1\,(\mathrm{kmol/m^3})^{(1-\alpha-\beta)}$, E^* is the activation energy, T^* is the temperature, R is the universal gas constant, ρ is the density, α and β are the reaction orders with respect to fuel and oxidizer, respectively. In the following, we will skip writing the unit conversion factor u. The energy equation in terms of temperature reads

$$mc_p\frac{dT^*}{dt^*} = \dot{m}c_p(T_u - T^*) - VQ^*\dot{\omega}_F \tag{8}$$

where Q^* is the heat of combustion per mole of fuel. There are two characteristic times in the system; the residence time t_m^*, which for the PSR can be expressed as

$$t_m^* = \frac{m}{\dot{m}} = \frac{\rho V}{\dot{m}} \tag{9}$$

and the chemical reaction time t_c^*, which can be expressed as $t_c^* = 1/A$. Following Oberlack et al. [3], a non-dimensionalization is introduced as

$$\begin{aligned} &Y_O = \frac{Y_O^*}{Y_{Ou}}, Y_F = \frac{Y_F^*}{Y_{Fu}}, T = \frac{T^*}{T_u}, \\ &t = \frac{t^*}{t_m^*}, E = \frac{E^*}{RT_u}, Q = \frac{Q^*Y_{Fu}}{W_F c_p T_u}, Da = At_m^* \end{aligned} \tag{10}$$

where $Da = t_m^*/t_c^*$ is the Damköhler number. Substitution of the non-dimensional variables to Eqs. (3), (4) and (8) leads to the following system of equations

$$\frac{dY_F}{dt} = 1 - Y_F - Da\frac{W_F}{\rho Y_{Fu}}\left(\frac{\rho Y_{Fu}Y_F}{W_F}\right)^{\alpha}\left(\frac{\rho Y_{Ou}Y_O}{W_O}\right)^{\beta}\exp\left(-\frac{E}{T}\right) \tag{11}$$

$$\frac{dY_O}{dt} = 1 - Y_O - Da\frac{\nu W_O}{\rho Y_{Ou}}\left(\frac{\rho Y_{Fu}Y_F}{W_F}\right)^{\alpha}\left(\frac{\rho Y_{Ou}Y_O}{W_O}\right)^{\beta}\exp\left(-\frac{E}{T}\right) \tag{12}$$

$$\frac{dT}{dt} = 1 - T + Da\frac{QW_F}{\rho Y_{Fu}}\left(\frac{\rho Y_{Fu}Y_F}{W_F}\right)^{\alpha}\left(\frac{\rho Y_{Ou}Y_O}{W_O}\right)^{\beta}\exp\left(-\frac{E}{T}\right) \tag{13}$$

2.1. Assumption of lean combustion

In this section, we present the analysis of the above-derived equations leading to the results obtained by Oberlack et al. [3], which can be considered as a special case of our generalized method presented in the following section (Section 2.2). Oberlack et al. assumed that the combustion is lean, and the rate of reaction is first order with respect to fuel. This is equivalent to taking $\alpha = 1$ and $\beta = 0$ in Eqs. (11)–(13). In such a case there is no need to track the oxidizer and the set of Eqs. (11)–(13) reduces to

$$\frac{dY_F}{dt} = 1 - Y_F - DaY_F \exp\left(-\frac{E}{T}\right) \tag{14}$$

$$\frac{dT}{dt} = 1 - T + DaQY_F \exp\left(-\frac{E}{T}\right) \tag{15}$$

At equilibrium, where the left-hand side derivatives are zero, the equations can be rearranged to give

$$T = 1 + Q(1 - Y_F) \tag{16}$$

or

$$Y_F = \frac{1 + Q - T}{Q} \tag{17}$$

which upon substitution to the energy Eq. (15) reads

$$\frac{dT}{dt} = 1 - T + Da(1 + Q - T) \exp\left(-\frac{E}{T}\right) \tag{18}$$

Utilizing the steady state assumption again by taking $dT/dt = 0$, Eq. (18) can be written as

$$1 - T + Da(1 + Q - T) \exp\left(-\frac{E}{T}\right) = 0 \tag{19}$$

which is convenient to rewrite as

$$Da(T) = \frac{(T - 1) \exp\left(\frac{E}{T}\right)}{(1 + Q - T)} \tag{20}$$

In Fig. 1 the $Da(T)$ function, as defined in Eq. (20), is plotted for constant $Q = 2$ and selected values of E. The function has two extrema for large E, which indicate the existence of two stable solutions (and one unstable solution) for a given Damköhler number Da. The two extrema correspond to ignition and extinction. Mathematically, the transition points from stable to unstable solution ('Ig' in Fig. 1), and from unstable to stable solution ('Ex' in Fig. 1) constitute saddle-node bifurcations. Under certain conditions (for $E = 6$ in the figure), when these two points meet, a cusp bifurcation occurs, and the function becomes monotonic. This allows for obtaining one solution from the $Da(T)$ curve and indicates a smooth transition between unburned and burned states, in which ignition and extinction events are suppressed. For smaller values of E the function remains monotonic. Oberlack et al. [3] identified this change of behavior, in which the solution depends monotonically on Da, as the MILD combustion. By analyzing the real solutions at the extrema of the $Da(T)$ curve obtained by taking $dDa/dT = 0$, they found that the transition to the monotonic function (i.e. to MILD combustion) occurs when

$$E = \frac{4(1 + Q)}{Q} \tag{21}$$

and the corresponding dimensionless temperature is

$$T = \frac{2(1 + Q)}{2 + Q} \tag{22}$$

The MILD combustion regime is obtained when E is smaller or equal to that obtained from Eq. (21), i.e. $E \leq 4(1 + Q)/Q$, see Oberlack et al. [3] for a more detailed discussion. It is also worth mentioning that due to the adopted assumption that the reaction rate terms are calculated based on the mixed quantities, besides the above condition for MILD combustion, the prerequisite condition is that the mixing time must be shorter than the reaction time.

2.2. A more general approach

If the assumption of lean combustion is not made, the set of Eqs. (11)–(13) has to be analyzed together. Making use of the steady state assumption, i.e. taking $dT/dt = dY_F/dt = dY_O/dt = 0$, and introducing an expression for the exponential term in Eq. (11) into Eq. (12) one obtains

$$Y_O = 1 - (1 - Y_F)\frac{Y_{Fu}\nu W_O}{Y_{Ou}W_F} \tag{23}$$

Furthermore, substituting the mass balance for the fuel in Eq. (11) into the energy Eq. (13) one obtains

$$Y_F = 1 + (1 - T)\frac{c_p T_u W_F}{Q^* Y_{Fu}} = \frac{1 + Q - T}{Q} \tag{24}$$

Then, substituting Eq. (24) into Eq. (23) leads to

$$Y_O = 1 + (1 - T)\frac{c_p T_u \nu W_O}{Q^* Y_{Ou}} = 1 + \frac{(1 - T)}{Q}\frac{Y_{Fu}\nu W_O}{Y_{Ou}W_F} \tag{25}$$

Eqs. (24) and (25) define the algebraic coupling between fuel and oxidizer concentrations with temperature. Substituting both (24) and (25) into (13) gives

$$\begin{aligned}\frac{dT}{dt} = 1 - T + \frac{DaQW_F}{\rho Y_{Fu}}&\left[\frac{\rho Y_{Fu}}{W_F}\left(1 + \frac{(1 - T)}{Q}\right)\right]^{\alpha} \\ &\cdot \left[\frac{\rho Y_{Ou}}{W_O}\left(1 + \frac{(1 - T)}{Q}\frac{Y_{Fu}\nu W_O}{Y_{Ou}W_F}\right)\right]^{\beta} \exp\left(-\frac{E}{T}\right)\end{aligned} \tag{26}$$

Using the following substitutions

$$c_{Fu} = \frac{\rho Y_{Fu}}{W_F} \tag{27}$$

$$c_{Ou} = \frac{\rho Y_{Ou}}{W_O} \tag{28}$$

$$\phi = \frac{Y_{Fu}\nu W_O}{Y_{Ou}W_F} \tag{29}$$

where ϕ is the equivalence ratio, and c_{Fu} and c_{Ou} are the molar concentrations of fuel and oxidizer at the unburned state, the equation simplifies to

$$\begin{aligned}\frac{dT}{dt} = 1 - T + \frac{DaQ}{c_{Fu}}&\left[c_{Fu}\left(1 + \frac{(1 - T)}{Q}\right)\right]^{\alpha} \cdot \\ &\cdot \left[c_{Ou}\left(1 + \frac{(1 - T)}{Q}\phi\right)\right]^{\beta} \exp\left(-\frac{E}{T}\right)\end{aligned} \tag{30}$$

For the steady state solution $dT/dt = 0$, the equation can be rewritten as

$$Da = \frac{(T - 1)c_{Fu} \exp\left(\frac{E}{T}\right)}{Q\left[c_{Fu}\left(1 + \frac{(1-T)}{Q}\right)\right]^{\alpha}\left[c_{Ou}\left(1 + \frac{(1-T)}{Q}\phi\right)\right]^{\beta}} \tag{31}$$

Eq. (31) is the final form which links the Damköhler number with dimensionless temperature T and depends on the inlet (unburned) quantities, i.e. equivalence ratio ϕ, and concentrations of fuel and oxidizer, but is independent of Y_F and Y_O. One can easily verify that by substituting $\alpha = 1$ and $\beta = 0$ into Eq. (31), this equation simplifies, as expected, to the final result of Oberlack et al. given in Eq. (20). It can also be deduced from Eq. (31) that, in the limit as $\phi \to 0$, when the oxidizer is abundant, $\beta = 0$ and Eq. (31) simplifies to

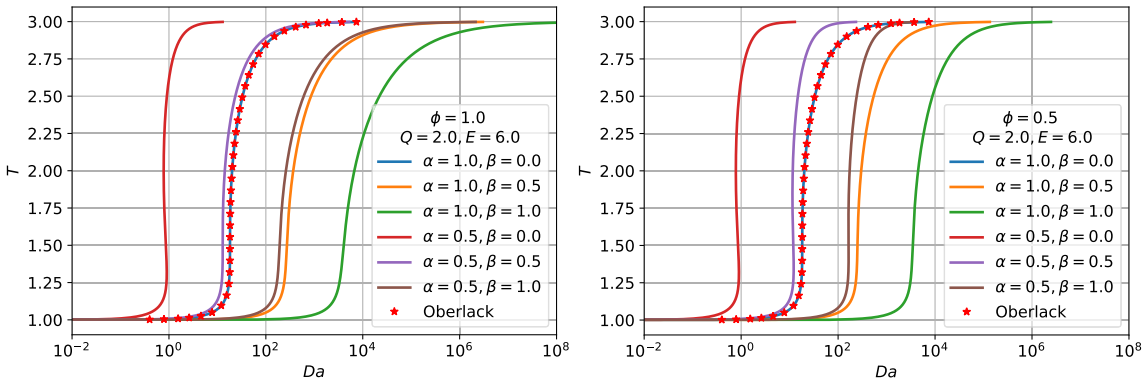

Fig. 2. Comparison of the S-shaped curves obtained from Eq. (31) with the solution of Oberlack et al. [3] Eq. (20), and the effect of varying the equivalence ratio ϕ and reaction orders α and β on their shape. The results were obtained for $c_{Fu} = 3$ mol/m^3 and $c_{Ou} = 6$ mol/m^3.

$$Da = \frac{(T-1)c_{Fu}^{1-\alpha}\exp\left(\frac{E}{T}\right)}{Q\left(1+\frac{(1-T)}{Q}\right)^{\alpha}} \tag{32}$$

In the rich limit, when $\phi \to \infty$, $\alpha = 0$. Then, using the Eqs. (27)–(29) one obtains

$$Da = \frac{(T-1)c_{Fu}^{1-\beta}\exp\left(\frac{E}{T}\right)}{Q\left(\frac{\nu(1-T)}{Q}\right)^{\beta}} \tag{33}$$

It should be noted that complete combustion was assumed in the model; therefore, it is strictly valid for $\phi \leq 1$. The model can also be used in rich conditions, however, taking into account the fact that the stoichiometry of reaction (1) may change and the heat of reaction Q^* decreases due to incomplete combustion. Therefore, in rich conditions, one may take into account this fact, for example by reducing Q^* to compensate for the error resulting or by accepting the error.

In Fig. 2 S-shaped curves obtained from Eq. (31) are compared with the results of Oberlack et al. [3] as given by Eq. (20). The effect of the equivalence ratio ϕ and the reaction orders α and β is also presented. As expected, the results coincide for $\alpha = 1$ and $\beta = 0$. As α and β increase, the solution shifts towards higher values of Da. The influence of the equivalence ratio ϕ on the results is such that the greater ϕ is, the greater the Da number. This influence occurs only for nonzero β and increases as T rises. It can also be concluded from the presented results that the highest influence on E occurs for $\phi = 1$, but as will be shown later, the influence is even greater under rich conditions, when $\phi > 1$.

3. Calculation procedure and validation

As mentioned in Section 2.1, the inflection point of the $Da(T)$ curve, arising from the coincidence of the turning points and defining the beginning of MILD combustion, comprises a cusp bifurcation. Therefore, the condition for the inflection point is that the first and second derivatives of Da with respect to T must be 0, and the third derivative cannot vanish; therefore, it can be written as

$$\frac{dDa}{dT} = 0, \quad \frac{d^2Da}{dT^2} = 0, \quad \frac{d^3Da}{dT^3} \neq 0 \tag{34}$$

The derivatives of Da (Eq. 31) with respect to T can be determined analytically. The first two derivatives have the form

$$\begin{aligned}\frac{dDa}{dT} = &-\frac{c_{Fu}^2 c_{Ou}\exp\left(\frac{E}{T}\right)}{Q^3T^2}\left[\frac{c_{Fu}(1-T+Q)}{Q}\right]^{-\alpha-1}\cdot\\ &\cdot\left[\frac{c_{Ou}(\phi(1-T)+Q)}{Q}\right]^{-\beta-1}\left[\alpha(T-1)T^2(\phi(T-1)-Q)+\right.\\ &\left.-(1-T+Q)(\beta\phi(T-1)T^2+(E(T-1)-T^2)(\phi(T-1)-Q))\right]\end{aligned} \tag{35}$$

$$\begin{aligned}\frac{d^2Da}{dT^2} = &\frac{c_{Fu}\exp\left(\frac{E}{T}\right)}{Q}\left(\frac{c_{Fu}(1-T+Q)}{Q}\right)^{-\alpha}\left(\frac{c_{Ou}(\phi(1-T)+Q)}{Q}\right)^{-\beta}\cdot\\ &\cdot\left[\frac{2\alpha\beta\phi(T-1)}{(Q-T+1)(\phi(1-T)+Q)}-\frac{2\alpha E(T-1)}{T^2(Q-T+1)}+\frac{\alpha(\alpha+1)(T-1)}{(Q-T+1)^2}+\right.\\ &+\frac{2\alpha}{Q-T+1}-\frac{2\beta E\phi(T-1)}{T^2(\phi(1-T)+Q)}+\frac{\beta(\beta+1)\phi^2(T-1)}{(\phi(1-T)+Q)^2}+\\ &\left.+\frac{2\beta\phi}{\phi(1-T)+Q}+\frac{E^2(T-1)}{T^4}+\frac{2\,E(T-1)}{T^3}-\frac{2\,E}{T^2}\right]\end{aligned} \tag{36}$$

Application of conditions (34) to the derivatives (35) and (36) leads to a set of 2 non-linear equations, where the sought-for variables are E and T, which can be found numerically for a given set of Q, c_{Fu}, c_{Ou}, α, β and ϕ. The solutions, i.e. roots of derivatives, were found using modified Powell's hybrid method of the 'root' function ('hybr' method) implemented in the 'SciPy optimize' package [21]. The modified Powell's hybrid method is a SciPy implementation of this algorithm from MINPACK [22] package for solving systems of nonlinear equations. The Jacobian required during the solution was computed by the algorithm using either the update formula of Broyden or forward-difference approximation. The convergence was controlled by a user-supplied tolerance *xtol* used to estimate the distance between the actual solution and the current approximation of the solution, which we set to 10^{-13}. The maximum number of calls to the function 'maxfev' was set to 10^4. All other solver options remained unchanged, including the 'eps' parameter used to calculate the forward-difference approximation of the Jacobian (set to machine precision by default). To perform the calculations, it was necessary to assume appropriate initial guesses for T and E. The initial values depend on the other parameter values, i.e. ϕ, α, β, and Q. Since we started the calculations with small values of Q, α and β, $T = 1.1$ was assumed and E ranged from 10 to 24, depending on β (higher initial E for higher β was required). In the examples presented in Section 4.2, the calculations were started with the largest values of Q. In the subsequent increments of Q, the results from the previous solution were used as initial values. The Levenberg-Marquardt method available in SciPy's 'root' function was also tested and gave the same results as the modified Powell's hybrid method. Another possible and elegant way to solve this problem is to apply the numerical continuation method. Analyzing the given expressions for the derivatives, one can see that the solution for criterion (34) is influenced only by the last terms of the products on the right-hand sides of Eqs. (35) and (36). The reason for this is that the first three factors can never be zero for physical solutions. In our calculations, in some cases we omitted the $\exp(E/T)$ term, whose removal improved the stability of the solution for small values of Q. In most cases, removing this term was not necessary. To validate the proposed approach, the methodology was first applied to the Oberlack et al. [3] criterion, for which the analytical solution is known. In Fig. 3 the Oberlack's criterion

(21) (analytical Oberlack) is compared with the numerical solution obtained by finding the roots of the first two derivatives of (20) (numerical Oberlack) and the derivatives given by Eqs. (35) and (36) for $\alpha = 1$ and $\beta = 0$ (numerical this work). As can be seen, all the results (all three $E(Q)$ curves) coincide, and therefore it was confirmed that for $\alpha = 1$ and $\beta = 0$ the derivatives (35) and (36) simplify to the solution of Oberlack, and it was concluded that the methodology was validated and ready to be applied to solve Eqs. (34)–(36) under other conditions.

To compare the results with other MILD combustion definitions, the procedure presented in [4] and [5] was used, in which the different definitions can be compared in the diagram $\Delta T/T_u$ vs. T_u. Here ΔT is the temperature increase in an adiabatic combustor. It can be shown that for the energy balance of such a chamber with assumed constant average specific heats and the same unburned temperatures of fuel, oxidizer and diluent, the ratio $\Delta T/T_u = Q$. In Fig. 4, four different MILD combustion regime boundaries according to the definitions of Oberlack et al. [3] (premixed), Cavaliere and de Joannon [4] (PSR), Evans et al. [5] (non-premixed), and this work (premixed) for various equivalence ratios ϕ, are shown. The MILD combustion regions lie under the curves (between the top and bottom curves for the model of Evans et al.). The self-ignition temperature for the model of Cavaliere and de Joannon was $T_{si} = 800$ K. For the other models, the activation energy was $E^* = 2.02 \times 10^8$ J/kmol, and the reaction orders were $\alpha = 0.2$, $\beta = 1.3$ for CH_4 [23]. Additionally, for the model of Evans et al. [5] the $T_{st,u} = T_u$. The results obtained for the Oberlack et al., Cavaliere and de Joannon and Evans et al. models reproduce the results obtained in [5] (for slightly different data). They also show good qualitative agreement with the model introduced in this work, and quantitatively illustrate the effect of the kinetic parameters and the equivalence ratio on the results. An increase in the equivalence ratio results in a larger temperature increase $\Delta T/T_u$, for the same inlet/unburned temperature T_u, which is consistent with intuition and the energy balance, and means that increasing ϕ, increases the region of MILD combustion. The calculations for rich conditions did not take into account the effect of the decrease in the heat of combustion, which will be discussed in more detail later in this work. A broader discussion on the interpretation of the results for the Oberlack et al., Cavaliere and de Joannon and Evans et al. models can be found in the work [5]. From the obtained results, it can be concluded that the model presented in this work predicts trends consistent with the Oberlack et al. model, while allowing for the inclusion of the influence of the kinetic parameters α, β and equivalence ratio ϕ on the location of the MILD combustion boundary.

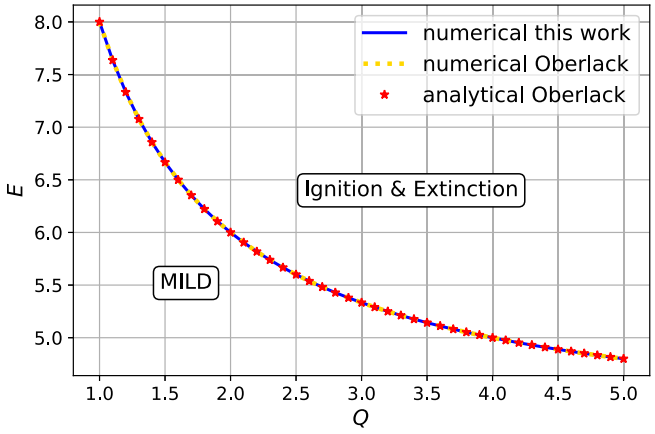

Fig. 3. The values of E and Q defining the MILD combustion limit obtained by solving Eq. (21) (analytical Oberlack) and by applying the proposed methodology of finding roots of the derivatives of Eq. (21) (numerical Oberlack) and roots of (35) and (36) with $\alpha = 1$ and $\beta = 0$ (numerical this work).

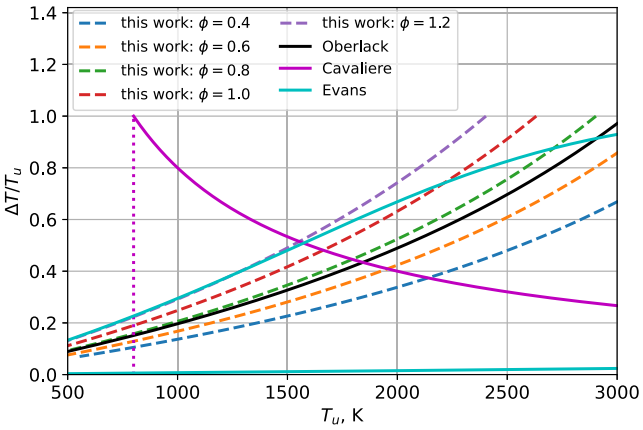

Fig. 4. Comparison of various regime boundaries of MILD combustion according to four different definitions: Oberlack et al. [3] (premixed), Cavaliere and de Joannon [4] (PSR), Evans et al. [5] (non-premixed), and this work for various equivalence ratios ϕ.

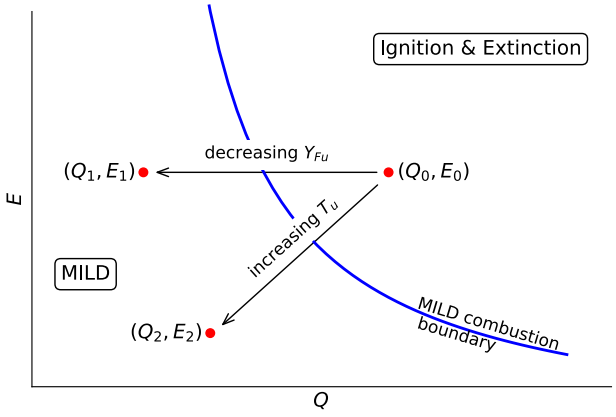

Fig. 5. Procedure for using the $E(Q)$ curve to identify the combustion regime for given T_u and Y_{Fu}.

3.1. Using the $E(Q)$ curves

To illustrate the procedure for using the determined $E(Q)$ curves, let us consider a situation in which the curve is already known. The method of its determination for a given fuel, i.e., for known Q^*, α, β, and E^* and the equivalence ratio ϕ was presented in the previous section (it will be discussed later that the MILD combustion boundary does not depend on c_{Fu} and c_{Ou}). In such a case, it is sufficient to determine/assume the temperature of the unburned mixture T_u and the mass fraction of the fuel Y_{Fu}, and using the relationships given by Eq. (10), $Q = Q^* Y_{Fu}/W_F c_p T_u$, $E = E^*/RT_u$ can be determined. Fig. 5 shows an example of the $E(Q)$ curve defining the MILD combustion boundary and an initial point (Q_0, E_0) in the *regular* combustion region, characterized by the existence of ignition and extinction solutions. To transition to the MILD combustion region, Q must be reduced, which can be achieved by reducing the mass fraction of fuel in the mixture Y_{Fu}. Then, the value of E does not change, and a transition to point (Q_1, E_1) occurs. It is also possible to transition from point (Q_0, E_0) by increasing the mixture temperature T_u. In this case, the values of E and Q decrease during the transition to the point (Q_2, E_2). In particular, for a given unburned gas temperature T_u, it is possible to find the maximum allowable fuel mass fraction to remain in the MILD regime (on the $E(Q)$ curve). Then, for a given $T_u = E^*/ER$, one obtains $Y_{Fu} = QW_F c_p E^*/ERQ^*$, where Q and E should be determined from the $E(Q)$ curve. It should also be emphasized that according to the above methodology of determining the MILD combustion boundary, the $E(Q)$ curve depends on the equivalence ratio

ϕ. Therefore, a given fuel mass fraction Y_{Fu} corresponds to one value of the oxygen mass fraction by Eq. (29), i.e. $Y_{Ou} = Y_{Fu}\nu W_O/\phi W_F$.

3.2. Mitigation of temperature overprediction

Under fuel-rich conditions ($\phi > 1$), combustible species are present in the combustion products. Neglecting this effect of incomplete combustion leads to an overprediction of the product temperature T^* if the heat of combustion Q^* is used in the model. Although the product species do not appear in the model, to account for the energy effects associated with all N combustible products, such as CO, H_2, etc., the heat of combustion Q^* can be reduced by:

$$\Delta Q^* = \sum_{i=1}^{N} \nu_i Q_i^* \tag{37}$$

where ν_i is the stoichiometric coefficient of the i-th product (per mole of fuel) and Q_i^* is the heat of combustion of the product species (per mole of product species). In general, the stoichiometric coefficients ν_i need to be calculated using temperature-dependent equilibrium constants or other equilibrium methods (if equilibrium can be assumed), or they represent the instantaneous composition of the reaction products at a given time (in non-equilibrium cases), which makes the formulation non-explicit. The determination of the composition of incomplete combustion products using equilibrium constants and other methods has been described in many combustion textbooks [2,24,25]. If, however, CO is assumed to be the only combustible compound formed during the incomplete combustion of a hydrocarbon fuel C_xH_y, its corresponding coefficient ν_{CO} can be calculated as:

$$\nu_{CO} = \frac{\phi - 1}{\phi}\left(2x + \frac{y}{2}\right) \tag{38}$$

Similarly, for incomplete combustion of H_2, where the only combustible product is H_2:

$$\nu_{H2} = \frac{\phi - 1}{\phi} \tag{39}$$

Regardless of the equivalence ratio, the energy balance of the process may also be affected by energy-consuming dissociation, which occurs at temperatures above approximately 1200 K [24]. If not accounted for, this effect can also lead to an overprediction of temperature. When chemical equilibrium can be assumed, the composition of the combustion products can be determined using equilibrium constants. In non-equilibrium cases, however, the product composition should be evaluated at a specific time instance. In both cases, Eq. (37) can be used to reduce the heat of combustion and correct the overprediction of temperature.

4. Results and discussion

A series of calculations were performed to examine the influence of the non-dimensional heat release Q, equivalence ratio ϕ and the reaction orders α and β on the non-dimensional activation energy E, which sets the upper limit of MILD combustion. In Fig. 6 sample results are presented for $\phi = 1$ and 0.5, and for $\alpha = 0.4$ and 1. As can be seen, whenever α or β or ϕ increases, $E(Q)$ increases. For $\alpha = 1$ and $\beta = 0$ the results coincide with the solution of Oberlack, as expected. This is true independently of the equivalence ratio. Interestingly, for stoichiometric conditions ($\phi = 1$), the results obtained also coincide with the solution of Oberlack whenever $\alpha + \beta = 1$. The reason for this reduction is that in this special case of $\alpha + \beta = 1$ and $\phi = 1$, it can be shown that the Eq. (31) simplifies to

$$Da = \frac{(T-1)\exp(E/T)}{(Q+1-T)}\nu^{\beta} \tag{40}$$

that differs from Oberlack's definition of Da (20) by the constant ν^{β}. This constant cancels out when the derivatives of $Da(T)$ are set to 0 to determine the MILD combustion limit. Furthermore, when $\beta < 1 - \alpha$, E is reduced w.r.t. the solution of Oberlack, and increases when $\beta > 1 - \alpha$. For ϕ other than 1, the latter rule is no longer true, and the results can coincide for various combinations of α and β. However, for a nonphysical value of $\phi = 0$ the solution reduces to the solution of Oberlack only when $\alpha = 1$, independently of β. It can also be noticed that the influence of the parameters studied on E is most pronounced for large ϕ. As ϕ decreases, the set of solutions is more compact and the results are closer to the solution of Oberlack. This is expected since the assumption of lean combustion made by Oberlack et al. [3] is associated with a decrease of ϕ (abundance of oxidizer), and it appears that it is less dependent on β as ϕ decreases. It should also be emphasized that the curves obtained that define the beginning of MILD combustion do not depend on c_{Fu} and c_{Ou}, although these quantities appear in the equations describing the derivatives (35) and (36). The reason for this lack of dependence can be found in the derivatives themselves, from which it follows that the only terms that can influence the result are the last factors in the Eqs. (35) and (36), because the first 3 factors of the product can never be 0, which is required to satisfy the conditions (34). As can be seen, c_{Fu} and c_{Ou} do not appear in them. At the same time, there is a relation between ϕ, c_{Fu} and c_{Ou} which follows from Eqs. (27)–(29)

$$\phi = \frac{c_{Fu}\nu}{c_{Ou}} \tag{41}$$

so the solution depends on ϕ in which the ratio of c_{Fu} and c_{Ou} is contained. As mentioned above, increasing ϕ shifts the MILD combustion boundary to higher values of E (besides the cases when $\beta = 0$), as can be seen in Fig. 6. Therefore, the model predicts a larger MILD region. If the unburned temperature T_u does not change and ϕ is increased, larger values of Y_{Fu} are allowed to remain in the MILD regime. Similarly, if the unburned fuel mass fraction Y_{Fu} is constant and ϕ increases, the model predicts that lower unburned temperatures T_u are allowed to remain in MILD regime, because both E and Q are inversely proportional to T_u. Similarly, increasing α and β shifts the MILD threshold to higher values of E. This behavior seems counterintuitive, as a reaction more sensitive to both reactants shifts the MILD combustion boundary upward, enlarging this region. It should be noted that variations in reaction orders are typically accompanied by corresponding changes in activation energy (change of fuel or applicability region). For more reactive fuels, the activation energy values of global reactions are usually lower than for less reactive fuels, which would suggest a lowering of the $E(Q)$ limit. However, determining the origin of this behavior requires further analysis of this model.

The observation that some of the solutions obtained for specific values of α and β (i.e. $\alpha + \beta = 1$ for $\phi = 1$) are reduced to the Oberlack solution allows for a convenient presentation of the obtained MILD combustion criteria in the form of the ratio E/E_O, where $E_O = 4(1+Q)/Q$ is the Oberlack criterion, as given in Eq. (21). In Fig. 7 the same results as presented in Fig. 6 are shown as the ratio of E/E_O. The E/E_O ratio is a constant function of 1 for the combinations of ϕ, α and β discussed above.

4.1. Results for a wide range of parameter variability

The above model and calculation methodology were used to perform a series of calculations for selected ranges of variability of the variables Q, ϕ, α and β. The ranges of these parameters were assumed taking into account the values of Q associated with common fuels ($Q \in [0.2, 6.5]$), and α and β that occur in global reaction mechanisms ($\alpha \in [0.2, 1.0]$, $\beta \in [0.0, 1.6]$), and for $\phi \in [0.2, 1.3]$. The kinetic parameters for the single-step reaction of various hydrocarbon fuels and two alcohols can be found in the work of Westbrook et al. [23]. For H_2 they are provided in the study of Marinov et al. [26], for CO in Dryer et al. [27], and for NH_3 in Yang et al. [28]. The results summarizing all calculated E/E_O

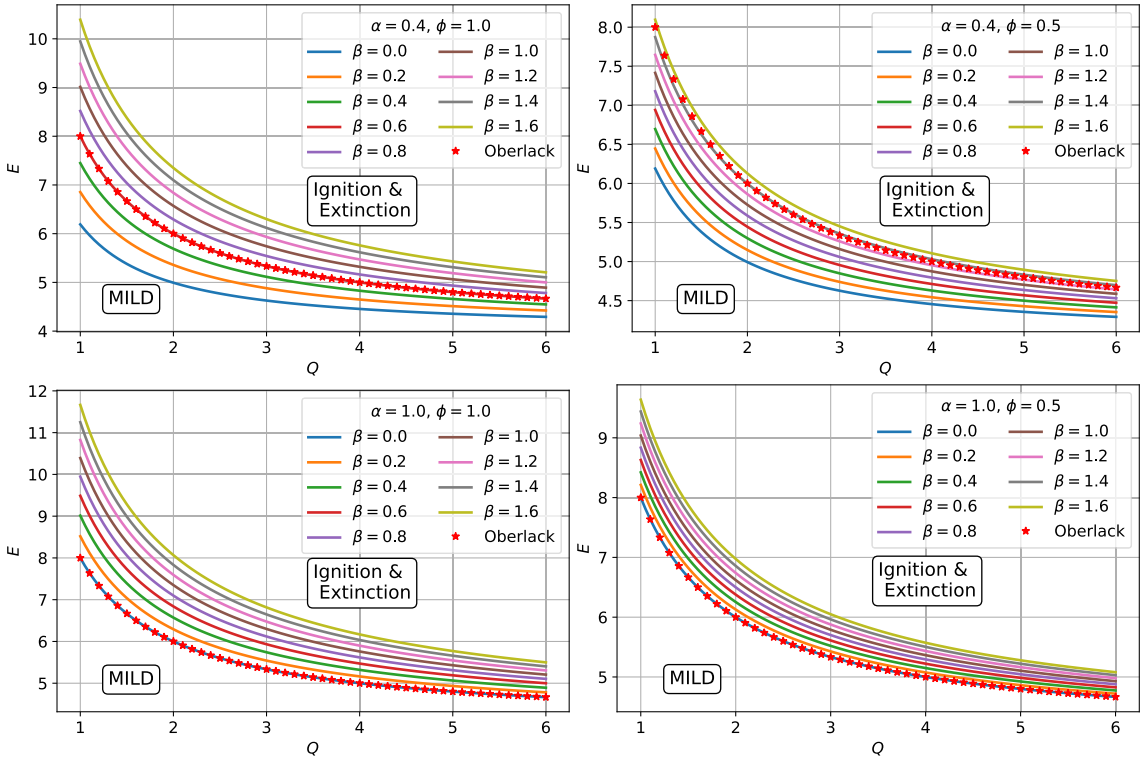

Fig. 6. The non-dimensional activation energy $E(Q)$ defining the MILD combustion boundary obtained for various β, $\alpha = 0.4$ and 1, for $\phi = 1$ (left panels) and $\phi = 0.5$ (right panels).

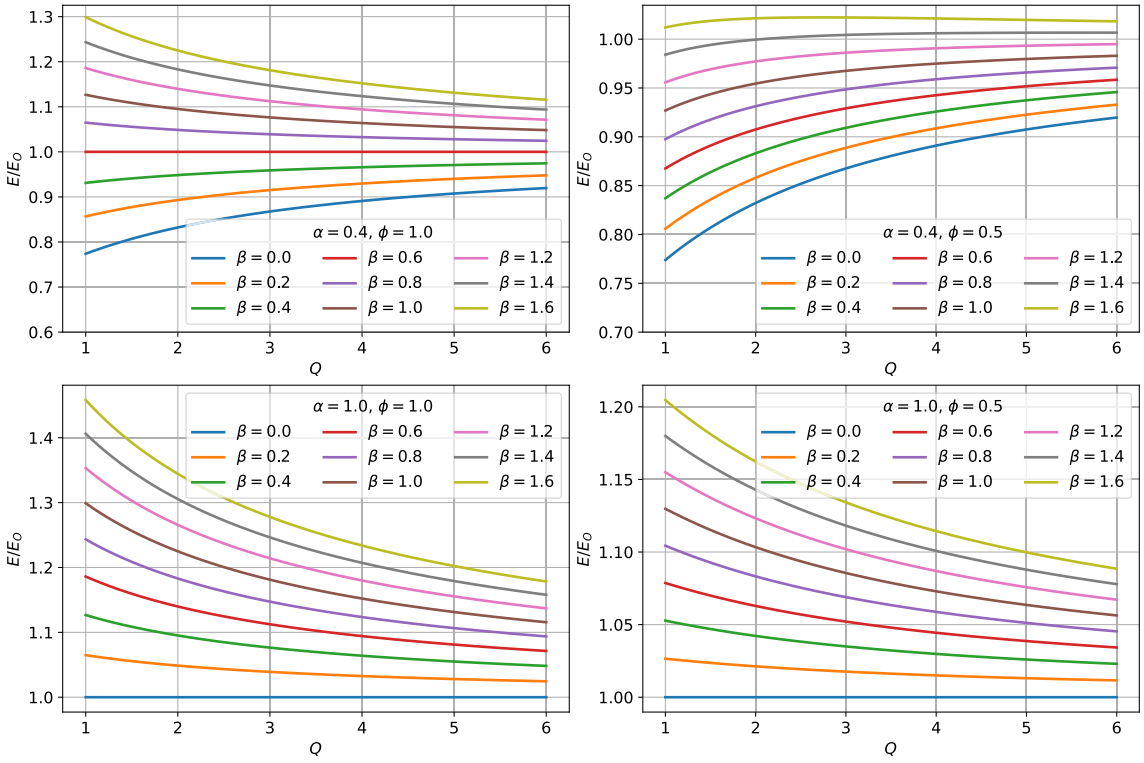

Fig. 7. The non-dimensional activation energy ratio E/E_O ratio vs Q defining the MILD combustion obtained for various β, $\alpha = 0.4$ and 1, for $\phi = 1$ (left panel) and $\phi = 0.5$ (right panel).

ratios are presented in Figs. 8–11. The presented results are general and can be used for various fuels and their corresponding global one-step reaction mechanisms. It should also be stressed that, in general, the overall reaction order $\alpha + \beta$ should not be greater than 2 [29], due to the requirement of reaction propagation. The presented results also cover situations where this condition is not met (i.e. in some plots $\alpha + \beta > 2$), which does not mean that it is physically justified. Furthermore, it is well known [23,25,30] that the flame speed S for most hydrocarbon fuels decreases with pressure p, and theoretical considerations showed that $S \sim p^{(\alpha+\beta-2)/2}$, which also leads to a limit on the value of the sum $\alpha + \beta$. In addition, the selected highest Q value was determined for stoichiometric ($\phi = 1$) combustion of hydrogen in air at $T_u = 300$ K. Such a high value at the MILD criterion is most likely unattainable for typical fuels, and smaller values of Q are expected, as will be shown below in the given numerical examples. To use the graphs in Figs. 8–11 for a given fuel for which Q^*, α, β, and E^* are known, one possible approach is to assume ϕ and find the appropriate graph and line corresponding to the value of β. Then, assuming T_u, E can be calculated, and additionally

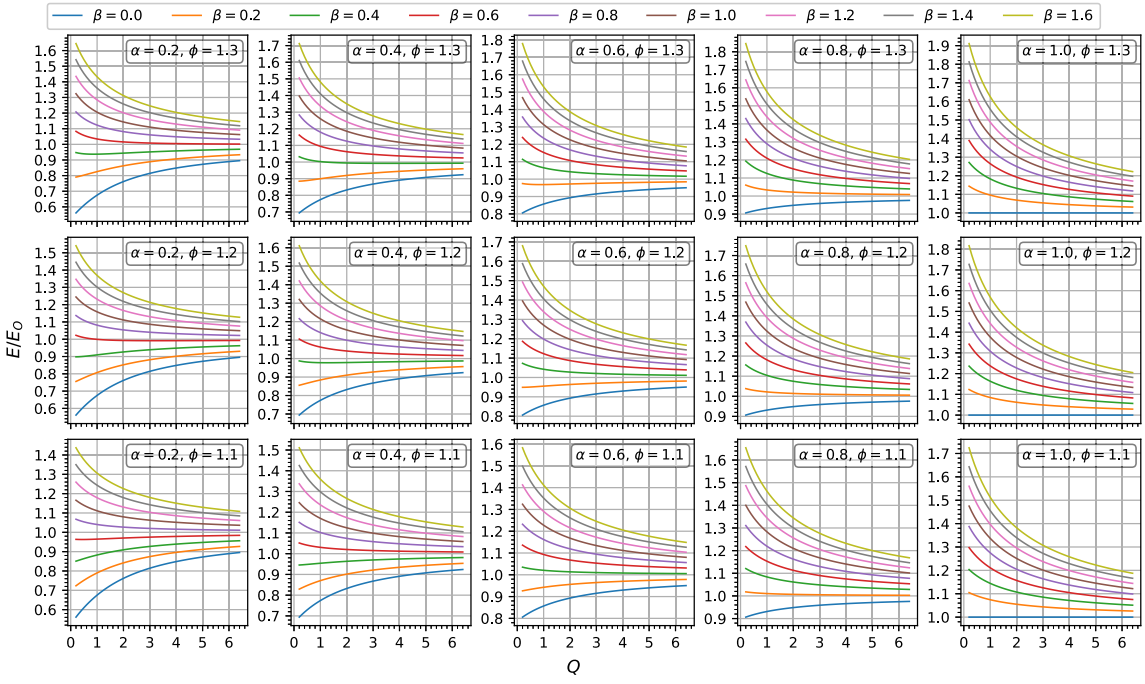

Fig. 8. The non-dimensional activation energy ratio E/E_O for equivalence ratio $\phi \in [1.1, 1.3]$.

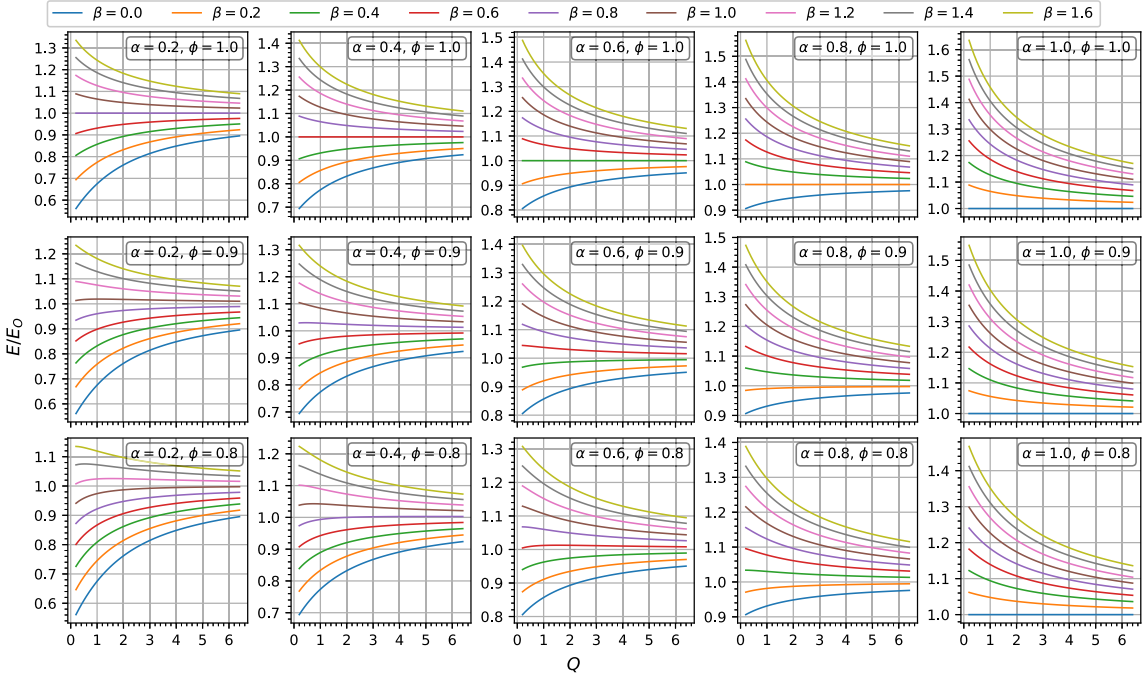

Fig. 9. The non-dimensional activation energy ratio E/E_O for equivalence ratio $\phi \in [0.8, 1.0]$.

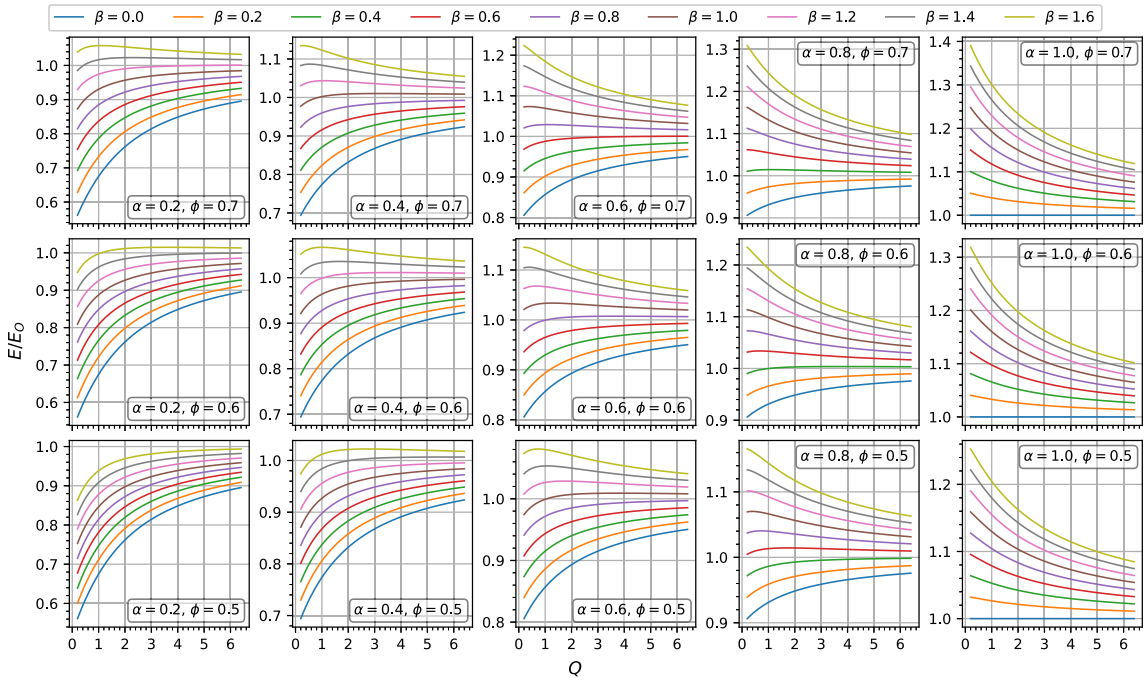

Fig. 10. The non-dimensional activation energy ratio E/E_O for equivalence ratio $\phi \in [0.5, 0.7]$.

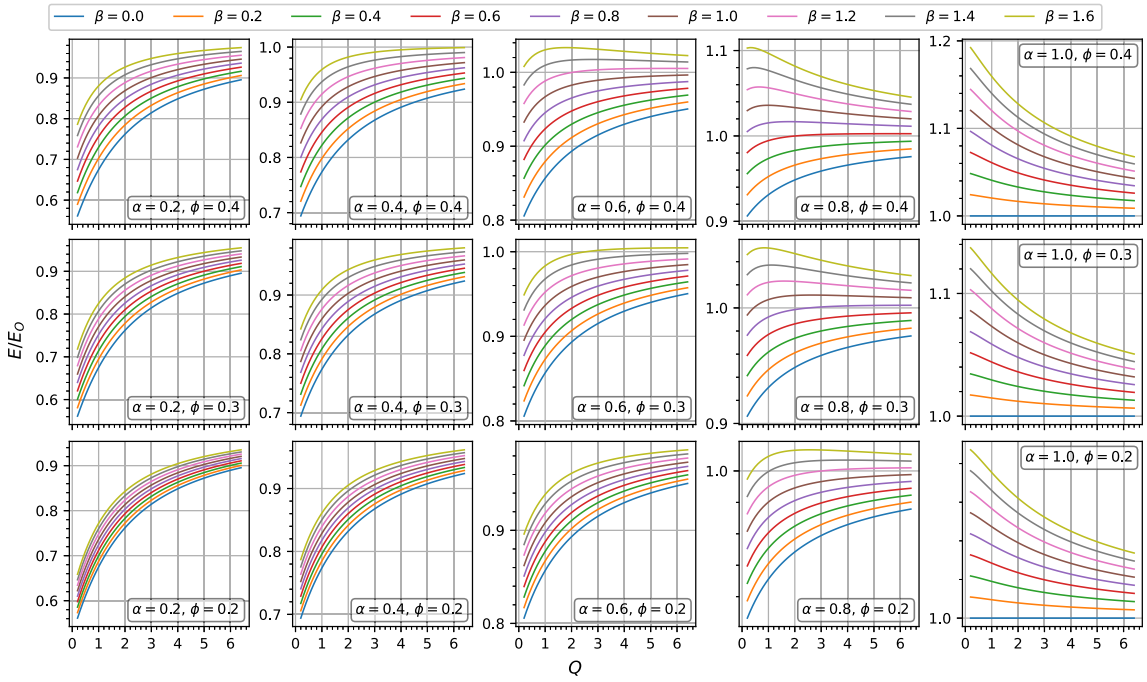

Fig. 11. The non-dimensional activation energy ratio E/E_O for equivalence ratio $\phi \in [0.2, 0.4]$.

assuming Y_{Fu}, Q, E_O and E/E_O can be calculated. The position relative to the boundary line can then be determined, thus the combustion regime can be identified. However, in order to find a more accurate position on the boundary line, T_u and/or Y_{Fu} must be selected, e.g. by trial and error.

It has also been verified that the condition that the third derivative of the Da number is different from zero is satisfied at the solution of $dDa/dT = 0$ and $d^2Da/dT^2 = 0$, see Eq. (34). The third derivative for all computed samples is presented in Fig. 12. As can be seen, all the third derivatives are nonzero at the solution, as required by the condition for the inflection point.

4.2. Numerical example for selected fuels

Here we present an example of applying the developed computational methodology for the case of hydrogen and methane combustion, in which the one-step global reactions are

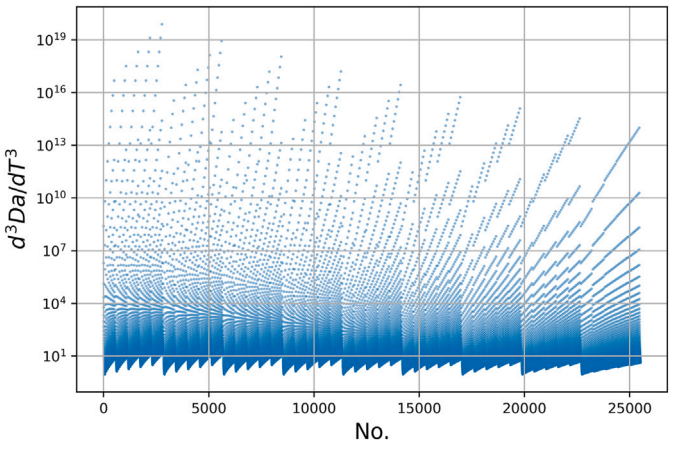

Fig. 12. The third derivative of Da w.r.t. T at the solution for all computed states.

Table 1
Kinetic parameters and lower heating value for hydrogen and methane.

Fuel	Q^*, MJ/kmol	E^*, J/kmol	α	β	Source
H_2	240.0	1.465×10^8	1.0	0.5	[26]
CH_4	802.3	2.025×10^8	0.2	1.3	[23]

$$H_2 + \frac{1}{2}O_2 \rightarrow H_2O \tag{42}$$

$$CH_4 + 2O_2 \rightarrow CO_2 + 2H_2O \tag{43}$$

The kinetic parameters for the reactions were taken from Marinov et al. [26] for hydrogen and Westbrook et al. [23] for methane. The values of the kinetic parameters and heating value Q^* are presented in Table 1.

The following procedure was applied to compute subsequent quantities:

- Choose the equivalence ratio ϕ, dimensionless heat of combustion Q and unburned gas specific heat c_p
- Calculate the dimensionless activation energy E and corresponding dimensionless temperature T for known α, β, Q and ϕ using Eq. (34)
- Knowing the dimensionless activation energy E calculate the unburned gas temperature as $T_u = E^*/ER$
- Calculate the unburned fuel mass fraction as $Y_{Fu} = QW_F c_p T_u/Q^*$
- Calculate the unburned oxygen mass fraction Y_{Ou} for the known Y_{Fu} and ϕ using $Y_{Ou} = Y_{Fu} n_{O2,\min} W_O/\phi W_F$, where $n_{O2,\min}$ is the minimum oxygen requirement expressed in moles of oxygen per mole of fuel

Figs. 13 and 14 show the results obtained after applying the above procedure for hydrogen and methane, respectively. In the left panels of the figures, the calculated dimensionless activation energy (indicating the upper boundary of MILD combustion region) and the corresponding temperature are presented for various Q and equivalence ratios ϕ. It should be noted that complete combustion was assumed in the model and a constant value of heat of combustion (lower heating value) Q^* was used also in rich conditions. Therefore, the presented results for $\phi > 1$ correspond to slightly higher values of Q than expected in reality, which also leads to higher predicted temperatures. A corrected (smaller) Q^* could be used to compensate for the error resulting from incomplete combustion. As can be seen, the influence of ϕ on E is significant and is much stronger for methane than for hydrogen. The highest values of E were obtained for $\phi = 1.2$, and gradually decreased with decreasing ϕ, which is in agreement with the previous results. For example, for methane and $Q = 0.1$ the value of E for $\phi = 1$ is 69 % higher than for $\phi = 0.4$. For hydrogen, the difference comprises only 15 %. The figures also show the result obtained using the Oberlack definition, which, for hydrogen, reaches the lowest values. This is consistent with the previously discussed lean combustion assumption, related to small ϕ. However, it should be noted that for methane the curve derived from the Oberlack criterion does not show this property, which is related to the very small α ($\alpha = 0.2$) reducing E. The left panels of the figures also show the nondimensional value of T corresponding to E, which limits the MILD combustion region. This temperature determines only the temperature value T for which the T vs. Da curves change from the S-curve with two turning points to the monotonic function with an inflection point. This value is therefore of rather informative importance, as it cannot be an indicator of MILD combustion by itself. The right panels of Figs. 13 and 14 show the corresponding temperature of the unburned gas ($T_u = E^*/ER$), as well as the mass fractions of fuel and oxygen. As Q increases, E decreases, which in turn leads to an increase in T_u, according to the definition of E in Eq. (10). The fuel mass fractions Y_{Fu} presented in the graphs are an important indicator of the given definitions of MILD combustion, as they inform what the maximum fuel mass fraction can be for a given temperature T_u so that the MILD combustion condition is met. Higher fuel mass fractions would lead to an increase in Q, which in turn would be associated with exceeding the MILD combustion limit (the E curve) and transitioning to combustion in which ignition and extinction occur. The corresponding mass fraction of oxygen Y_{Ou} plays the same role since it is linked to Y_{Fu} through $Y_{Ou} = Y_{Fu} n_{O2,\min} W_O/\phi W_F$. From the presented figures, it can also be concluded that for a constant temperature T_u, an increase in the value of ϕ causes an increase in the allowable mass fraction of fuel Y_{Fu} (the fraction of oxygen depends directly on ϕ). Moreover, for a constant fuel mass fraction Y_{Fu}, an increase in ϕ results in the possibility of maintaining MILD combustion at lower temperatures T_u.

4.3. Approximation

The general solutions presented in Figs. 9–11 can be approximated by fitting functions, which can be used in practical calculations and can easily be implemented in computational programs. For this purpose, the solutions obtained for $\phi \leq 1$ were approximated by combinations of polynomials (3rd order), power functions, and logarithms, as well as pure polynomials (4th order). The fitting of the approximation functions was performed using the 'curve_fit' function of the 'SciPy optimize' submodule [21] and Scikit-learn [31], respectively. The E/E_O ratio, where $E_O = 4(1+Q)/Q$, has been approximated with third and fourth-order polynomials with respect to α, β, and Q for various equivalence ratios ϕ. The approximation functions used are of the form

$$\begin{aligned} f_3(x,Q,n) &= (a_0x^3 + a_1x^2 + a_2x + a_3)\ln(a_4Q + a_5) + a_6Q^n + \\ &\quad + a_7x^3 + a_8x^2 + a_9x + a_{10} \\ x(\alpha,\beta) &= a_{11}\alpha + a_{12}\beta \\ n(\alpha,\beta) &= a_{13}\alpha + a_{14}\beta \end{aligned} \tag{44}$$

$$\begin{aligned} f_4(\alpha,\beta,Q) = {} & a_0 + a_1\alpha + a_2\beta + a_3Q + a_4\alpha^2 + a_5\alpha\beta + a_6\alpha Q + \\ & + a_7\beta^2 + a_8\beta Q + a_9Q^2 + a_{10}\alpha^3 + a_{11}\alpha^2\beta + a_{12}\alpha^2 Q + a_{13}\alpha\beta^2 + \\ & + a_{14}\alpha\beta Q + a_{15}\alpha Q^2 + a_{16}\beta^3 + a_{17}\beta^2 Q + a_{18}\beta Q^2 + a_{19}Q^3 + \\ & + a_{20}\alpha^4 + a_{21}\alpha^3\beta + a_{22}\alpha^3 Q + a_{23}\alpha^2\beta^2 + a_{24}\alpha^2\beta Q + a_{25}\alpha^2 Q^2 + \\ & + a_{26}\alpha\beta^3 + a_{27}\alpha x_1^2 Q + a_{28}\alpha\beta Q^2 + a_{29}\alpha Q^3 + a_{30}\beta^4 + a_{31}\beta^3 Q + \\ & + a_{32}\beta^2 Q^2 + a_{33}\beta Q^3 + a_{34}Q^4 \end{aligned} \tag{45}$$

A relatively high (3rd and 4th) order polynomials were chosen because a lower degree led to unsatisfactory accuracy. It was not possible to obtain accurate fitting functions with explicit dependency on the equivalence ratio. Instead, in Tables 2 and 3 different fitting coefficients

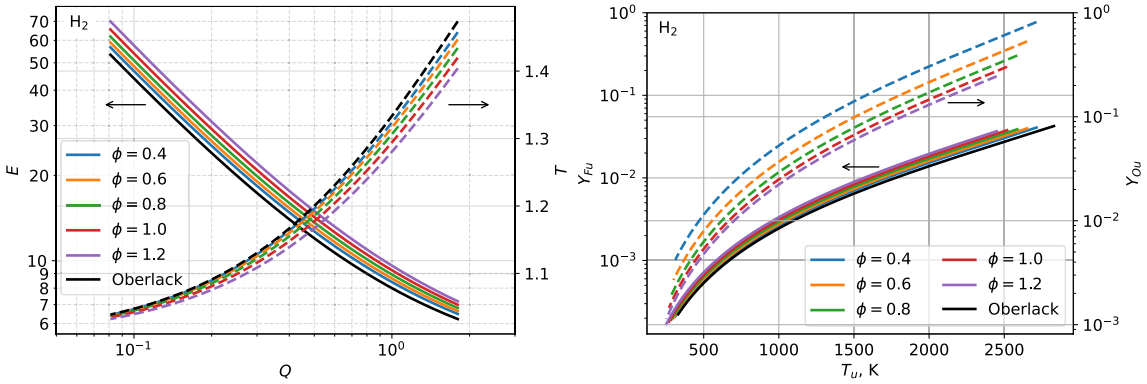

Fig. 13. The boundaries of MILD combustion region for hydrogen at various equivalence ratios (left panel). The corresponding unburnt fuel and oxygen mass fractions at unburnt temperatures T_u for $c_p = 1$ kJ/kgK (right panel).

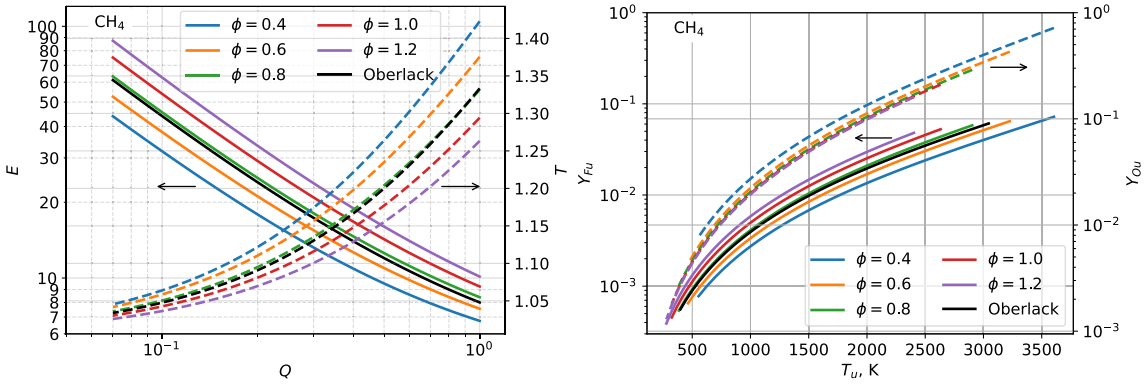

Fig. 14. The boundaries of MILD combustion region for methane at various equivalence ratios (left panel). The corresponding unburnt fuel and oxygen mass fractions at unburnt temperatures T_u for $c_p = 1$ kJ/kgK (right panel).

Table 2
Coefficients of function (44) for various equivalence ratios ϕ, valid for $\alpha \in [0.2, 1.0]$, $\beta \in [0.0, 1.6]$, $Q \in [0.2, 6.5]$.

ϕ	1	0.9	0.8	0.7	0.6	0.5	0.4	0.3
R^2	0.9998	0.9997	0.9997	0.9994	0.9988	0.9990	0.9986	0.9987
$RMSE$	1.859 E-03	2.184 E-03	2.060 E-03	2.445 E-03	3.288 E-03	3.410 E-03	3.446 E-03	3.318 E-03
max δ_{rel}	2.398 E-02	2.056 E-02	2.733 E-02	3.475 E-02	6.716 E-02	7.150 E-02	7.098 E-02	5.200 E-02
a_0	−7.097569 E-03	−7.258785 E-01	−1.518350 E-02	2.659435 E+00	−3.656741 E-03	−8.117686 E-01	−1.280713 E+00	−1.085637 E-02
a_1	4.401653 E-02	9.551209 E-01	6.821748 E-02	2.166456 E+00	2.759087 E-02	9.390432 E-01	1.264272 E+00	5.343119 E-02
a_2	−2.005878 E-01	−8.853729 E-01	−3.128557 E-01	1.578165 E+00	−7.809036 E-02	−8.495989 E-01	−1.153465 E+00	−1.876438 E-01
a_3	1.799359 E-01	1.803519 E-01	1.750786 E-01	1.674327 E-01	1.529755 E-01	1.651585 E-01	1.706141 E-01	1.727987 E-01
a_4	1.691307 E-01	1.747011 E+00	2.148574 E+00	1.803302 E+01	2.240006 E+00	8.041300 E+00	9.868582 E+00	4.269684 E+00
a_5	6.016567 E-02	6.009024 E-01	6.074521 E-01	3.439178 E+00	1.151750 E-01	1.123001 E+00	1.663198 E+00	6.965997 E-01
a_6	3.892238 E-03	2.965708 E-04	5.814726 E-01	1.718066 E+01	−7.118690 E-01	−4.776935 E-02	6.279207 E+01	−3.702090 E-02
a_7	−7.613530 E-05	1.652643 E+00	4.325570 E-02	−1.349822 E+01	1.156019 E-02	3.423229 E+00	5.639438 E+00	3.735653 E-02
a_8	−1.329090 E-02	−2.438019 E+00	−2.128220 E-01	−1.123934 E+01	−8.299950 E-02	−4.035597 E+00	−5.706304 E+00	−1.885953 E-01
a_9	1.331167 E-01	2.678114 E+00	8.862427 E-01	−8.017214 E+00	4.215673 E-01	3.876903 E+00	5.056090 E+00	7.261248 E-01
a_{10}	8.528149 E-01	4.353416 E-01	−1.705985 E-01	−1.710588 E+01	1.172121 E+00	2.667654 E-01	−6.262897 E+01	3.361886 E-01
a_{11}	1.161758 E+00	2.611313 E-01	8.951512 E-01	−1.609752 E-01	1.434429 E+00	2.623399 E-01	2.434479 E-01	1.320079 E+00
a_{12}	1.161528 E+00	2.247740 E-01	6.459101 E-01	−9.630859 E-02	6.947905 E-01	1.018225 E-01	7.032864 E-02	2.755930 E-01
a_{13}	6.021491 E-01	8.016361 E-01	8.341232 E-02	2.072110 E-03	1.117986 E-01	−1.036252 E-01	7.166367 E-04	−8.274036 E-02
a_{14}	6.136727 E-01	1.103353 E+00	6.825795 E-02	1.662937 E-03	4.419714 E-02	−2.811698 E-01	3.357059 E-04	−2.632202 E-01

(a_0–a_{14} for f_3 and a_0–a_{34} for f_4) are given for different equivalence ratios. The tables also contain the coefficients of determination R^2, Root Mean Square Errors (RMSE) and maximum relative errors (δ_{rel}) for each function. A comparison of the fitting functions with the actual results, for selected cases, is presented in Figs. 15 and 16. In general, the approximation functions predict the true numerical results well. For the approximation function f_3, although the coefficient of determination R^2 was greater than 0.9986 in all cases, small local overfitting can be observed. The approximation was improved and overfitting was reduced when the 4th order polynomials were used. Then R^2 was greater than 0.9997 in all cases. However, this was achieved by making the model more complex and using a significant number of coefficients, totaling 35. The approximation functions can be used for a given fuel, where α and β are known and for a given equivalence ratio ϕ. Then the ratio E/E_O can be determined as a function of Q. If equivalence ratios other than those specified are needed, one can interpolate between two E/E_O curves. The further procedure is analogous to the use of graphs of Figs. 8–11, which was described in Section 4.1.

Table 3
Coefficients of polynomial (45) for various equivalence ratios ϕ, valid for $\alpha \in [0.2, 1.0]$, $\beta \in [0.0, 1.6]$, $Q \in [0.2, 6.5]$.

ϕ	1.0	0.9	0.8	0.7	0.6	0.5	0.4	0.3
R^2	0.9997	0.9998	0.9998	0.9998	0.9998	0.9997	0.9997	0.9997
$RMSE$	2.239 E-03	1.777 E-03	1.518 E-03	1.451 E-03	1.487 E-03	1.522 E-03	1.496 E-03	1.395 E-03
max δ_{rel}	4.128 E-02	3.009 E-02	2.088 E-02	1.444 E-02	1.522 E-02	1.674 E-02	1.844 E-02	1.893 E-02
a_0	4.175398 E-01	4.046031 E-01	3.931589 E-01	3.835216 E-01	3.759052 E-01	3.703875 E-01	3.668813 E-01	3.651387 E-01
a_1	7.456192 E-01	7.699584 E-01	7.950708 E-01	8.199138 E-01	8.433387 E-01	8.642224 E-01	8.817005 E-01	8.953751 E-01
a_2	7.194717 E-01	6.088748 E-01	5.059087 E-01	4.113949 E-01	3.260377 E-01	2.502396 E-01	1.839594 E-01	1.267002 E-01
a_3	1.744197 E-01	1.913051 E-01	2.059047 E-01	2.177896 E-01	2.266427 E-01	2.323425 E-01	2.350376 E-01	2.351489 E-01
a_4	−2.146670 E-01	−2.373919 E-01	−2.633827 E-01	−2.919733 E-01	−3.220789 E-01	−3.522332 E-01	−3.808927 E-01	−4.068679 E-01
a_5	−3.576551 E-01	−3.211350 E-01	−2.814389 E-01	−2.393333 E-01	−1.962385 E-01	−1.539945 E-01	−1.143963 E-01	−7.875968 E-02
a_6	−2.170007 E-01	−2.298835 E-01	−2.431259 E-01	−2.560036 E-01	−2.676524 E-01	−2.772014 E-01	−2.840003 E-01	−2.878066 E-01
a_7	−1.739061 E-01	−1.239737 E-01	−8.435352 E-02	−5.443518 E-02	−3.307447 E-02	−1.871256 E-02	−9.650989 E-03	−4.339079 E-03
a_8	−2.096311 E-01	−1.717194 E-01	−1.364389 E-01	−1.044365 E-01	−7.637813 E-02	−5.280352 E-02	−3.396987 E-02	−1.977303 E-02
a_9	−2.137165 E-02	−2.930185 E-02	−3.611241 E-02	−4.160412 E-02	−4.562845 E-02	−4.813260 E-02	−4.919847 E-02	−4.904306 E-02
a_{10}	6.494910 E-02	7.460021 E-02	8.658672 E-02	1.009287 E-01	1.173618 E-01	1.352493 E-01	1.537070 E-01	1.719052 E-01
a_{11}	1.408238 E-01	1.368754 E-01	1.301575 E-01	1.201122 E-01	1.066829 E-01	9.043973 E-02	7.239937 E-02	5.363460 E-02
a_{12}	3.321427 E-02	3.925346 E-02	4.628375 E-02	5.408725 E-02	6.225953 E-02	7.023075 E-02	7.740215 E-02	8.332464 E-02
a_{13}	1.259942 E-01	9.981973 E-02	7.560813 E-02	5.435793 E-02	3.682252 E-02	2.326861 E-02	1.344994 E-02	6.810747 E-03
a_{14}	5.409488 E-02	4.909448 E-02	4.293699 E-02	3.578313 E-02	2.805231 E-02	2.037275 E-02	1.341769 E-02	7.715250 E-03
a_{15}	3.241808 E-02	3.477841 E-02	3.719037 E-02	3.948575 E-02	4.145954 E-02	4.290725 E-02	4.368443 E-02	4.375235 E-02
a_{16}	4.309141 E-02	2.757406 E-02	1.658588 E-02	9.331156 E-03	4.880327 E-03	2.339703 E-03	9.947641 E-04	3.496627 E-04
a_{17}	2.630008 E-02	1.754594 E-02	1.069941 E-02	5.739600 E-03	2.502213 E-03	6.773261 E-04	−1.340155 E-04	−3.285032 E-04
a_{18}	3.177675 E-02	2.552641 E-02	1.966284 E-02	1.433777 E-02	9.716447 E-03	5.944196 E-03	3.105497 E-03	1.197973 E-03
a_{19}	−3.100745 E-04	1.237898 E-03	2.566975 E-03	3.639583 E-03	4.428159 E-03	4.924082 E-03	5.144970 E-03	5.134317 E-03
a_{20}	−8.482735 E-03	−1.001363 E-02	−1.205960 E-02	−1.469890 E-02	−1.795706 E-02	−2.176213 E-02	−2.595339 E-02	−3.035278 E-02
a_{21}	−2.117784 E-02	−2.199985 E-02	−2.246300 E-02	−2.229218 E-02	−2.126181 E-02	−1.929321 E-02	−1.647754 E-02	−1.299400 E-02
a_{22}	−4.792522 E-03	−5.830811 E-03	−7.153464 E-03	−8.767833 E-03	−1.063642 E-02	−1.266403 E-02	−1.471794 E-02	−1.667268 E-02
a_{23}	−2.620972 E-02	−2.274321 E-02	−1.888311 E-02	−1.485899 E-02	−1.098670 E-02	−7.559491 E-03	−4.752337 E-03	−2.617222 E-03
a_{24}	−1.018265 E-02	−1.028183 E-02	−1.008410 E-02	−9.501533 E-03	−8.508553 E-03	−7.169262 E-03	−5.620897 E-03	−4.019801 E-03
a_{25}	−1.394098 E-03	−1.821584 E-03	−2.327546 E-03	−2.891630 E-03	−3.474561 E-03	−4.021192 E-03	−4.474843 E-03	−4.794896 E-03
a_{26}	−1.652268 E-02	−1.176153 E-02	−7.873739 E-03	−4.926735 E-03	−2.863335 E-03	−1.525395 E-03	−7.214653 E-04	−2.826319 E-04
a_{27}	−9.081064 E-03	−7.204153 E-03	−5.389221 E-03	−3.753803 E-03	−2.403114 E-03	−1.392722 E-03	−7.127319 E-04	−3.056704 E-04
a_{28}	−2.268519 E-03	−2.066805 E-03	−1.767156 E-03	−1.379958 E-03	−9.401980 E-04	−5.043366 E-04	−1.353461 E-04	1.164267 E-04
a_{29}	−1.984907 E-03	−2.133710 E-03	−2.284692 E-03	−2.425182 E-03	−2.539750 E-03	−2.613354 E-03	−2.636018 E-03	−2.606191 E-03
a_{30}	−4.496232 E-03	−2.624949 E-03	−1.424292 E-03	−7.166495 E-04	−3.325737 E-04	−1.393831 E-04	−5.021766 E-05	−1.411191 E-05
a_{31}	−3.119957 E-03	−1.921105 E-03	−1.081860 E-03	−5.466948 E-04	−2.418547 E-04	−8.970357 E-05	−2.512057 E-05	−3.632060 E-06
a_{32}	−1.105669 E-03	−6.367064 E-04	−2.779041 E-04	−3.377474 E-05	1.022756 E-04	1.495978 E-04	1.368486 E-04	9.434521 E-05
a_{33}	−1.970120 E-03	−1.572022 E-03	−1.195506 E-03	−8.519215 E-04	−5.539406 E-04	−3.130687 E-04	−1.364364 E-04	−2.456190 E-05
a_{34}	1.759761 E-04	7.027949 E-05	−2.063264 E-05	−9.428979 E-05	−1.489240 E-04	−1.840635 E-04	−2.009889 E-04	−2.026735 E-04

5. Model applicability

The solution and criterion obtained by Oberlack et al. [3] given by Eqs. (20) and (21), as well as in this work (31), are based on the same assumptions of a perfectly stirred reactor and a one-step reaction. These assumptions limit the applicability of these models because the assumed perfect mixing of the reactants, and therefore, the mixing time is infinitely short, and the composition and temperature are uniform within the entire system.

This means that in practice, the mixing time should be shorter than both the residence time (9) and the reaction time. At the same time, various values of the Damköhler number defined in Eq. (10) are permissible, i.e., both smaller and larger than 1. Therefore, the model can be used in situations where the mixing rate significantly exceeds the reaction rate, for example in combustors with intense turbulent mixing and slow reactions, where the residence time is still longer than the mixing time. This is consistent with previous observations that MILD combustion occurs in regions with diluted reactants and distributed reaction zones characterized by reduced temperature and slower reactions. These conditions are characterized by Damköhler numbers (defined as the mixing time and reaction time), close to or smaller than 1. In the latter case, they can be considered favorable for the assumption of a short mixing time in the PSR. In addition, the homogeneity of the concentration and temperature fields makes the model unsuitable for describing systems characterized by inhomogeneities, temperature gradients, or strong stratification.

The second important assumption of the model is the assumption of a one-step chemical reaction. As a result, based on the effective activation energy, this definition separates the conventional autoignitive combustion from gradually igniting MILD combustion. In this work, the influence of the reactants' concentrations and equivalence ratio is additionally included; however, the detailed reactions and the role of intermediate species and radicals are not. In particular, MILD combustion often occurs in the presence of recirculated exhaust gases, containing radicals that facilitate the initiation and propagation of the process. In this context, the possibility of representing the onset of this process using a single reaction with an effective activation energy raises concerns. As discussed in [17,32], the processes under MILD conditions cannot be represented without detailed modeling of the elementary reactions. A similar conclusion on the role of radicals was drawn by Ref. [33], who used the S-curve-based MILD definition of Evans et al. [5] in DNS studies of non-premixed flames. The above considerations suggest that both the model developed in this study and that proposed by Oberlack et al. [3] may have difficulties in predicting the actual conditions of MILD combustion due to the assumptions made. Therefore, preliminary results are presented below obtained using a PSR model with a GRI 3.0 mechanism, to verify the behavior of S-curves in the regions of 'regular combustion' and MILD combustion, as predicted by our model. The calculations were done using Cantera [34] code, and IdealGasReactor model for various residence times t_m^*, unburned temperatures T_u, and unburned fuel mass fraction Y_{Fu} for a given equivalence ratio ϕ. The calculations were performed independently for the upper and lower branches of the S-curve, assuming that the reactants were at T_u in the initial state (for the lower branch) and in the burned state, i.e., in equilibrium (for the upper branch). The calculations were performed using a transient solver, and integration continued until a steady state was reached. This approach was necessary due to the lack of a dedicated steady-state solver in

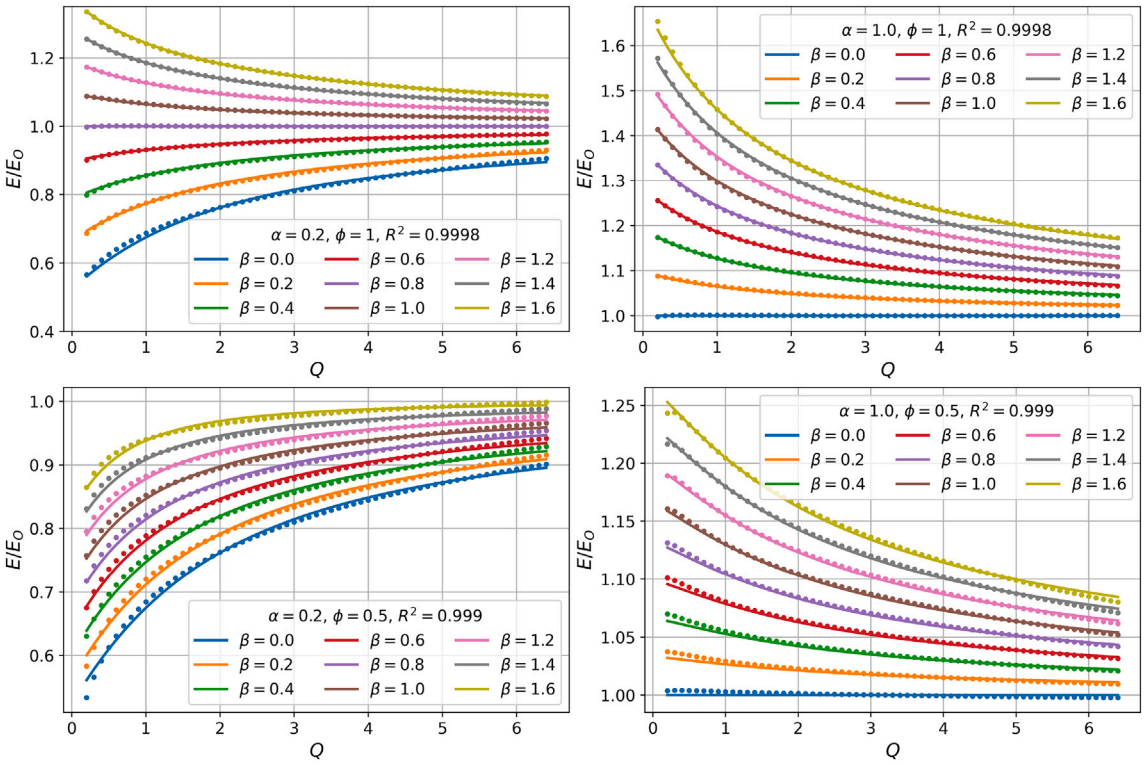

Fig. 15. The E/E_O ratio predicted by the approximation function (44) (dots) and the true result obtained from the numerical solution of (34) (solid lines) for selected α, β and ϕ.

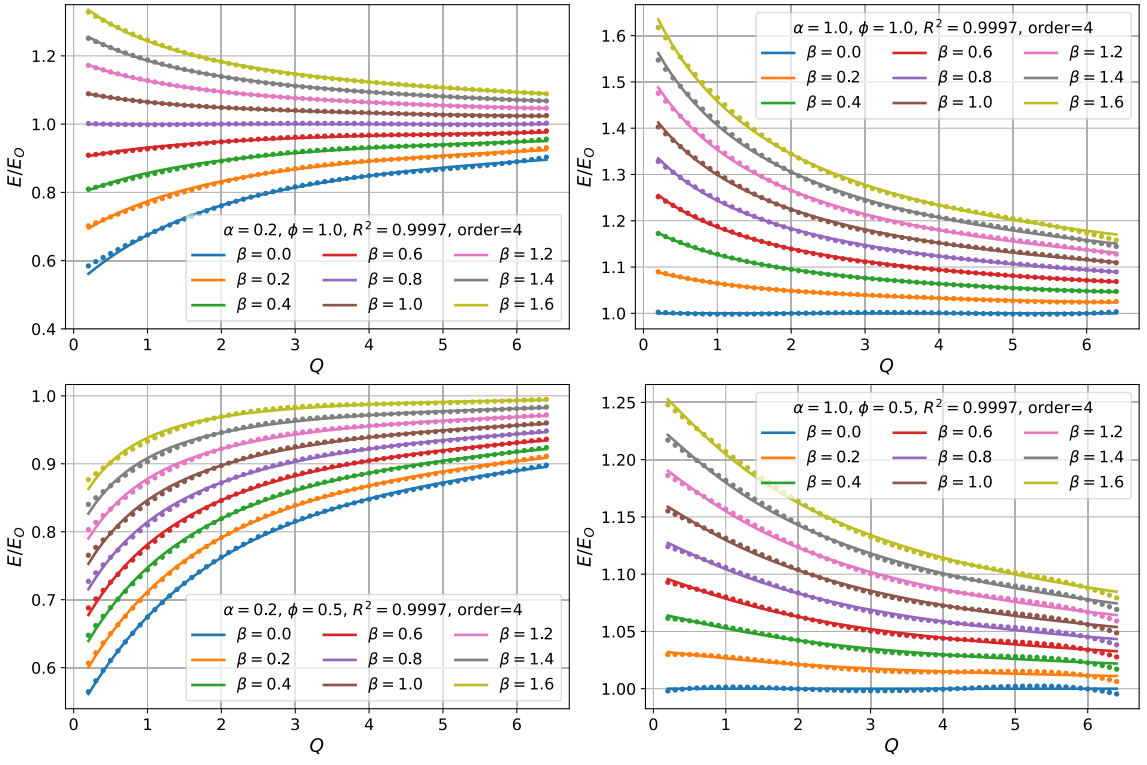

Fig. 16. The E/E_O ratio predicted by the approximation polynomials of 4th order (dots) and the true result obtained from the numerical solution of (34) (solid lines) for selected α, β and ϕ.

Cantera, which would otherwise be more suitable for this type of calculation. The method does not allow for predicting the unstable (middle) branch of the S-curve. Calculations were performed for a CH_4-O_2-N_2 mixture in which the fuel mass fraction Y_{Fu} and equivalence ratio ϕ were assumed, the mass fraction of oxygen was calculated according to Eq. (29), and nitrogen was calculated as the complement to unity. The

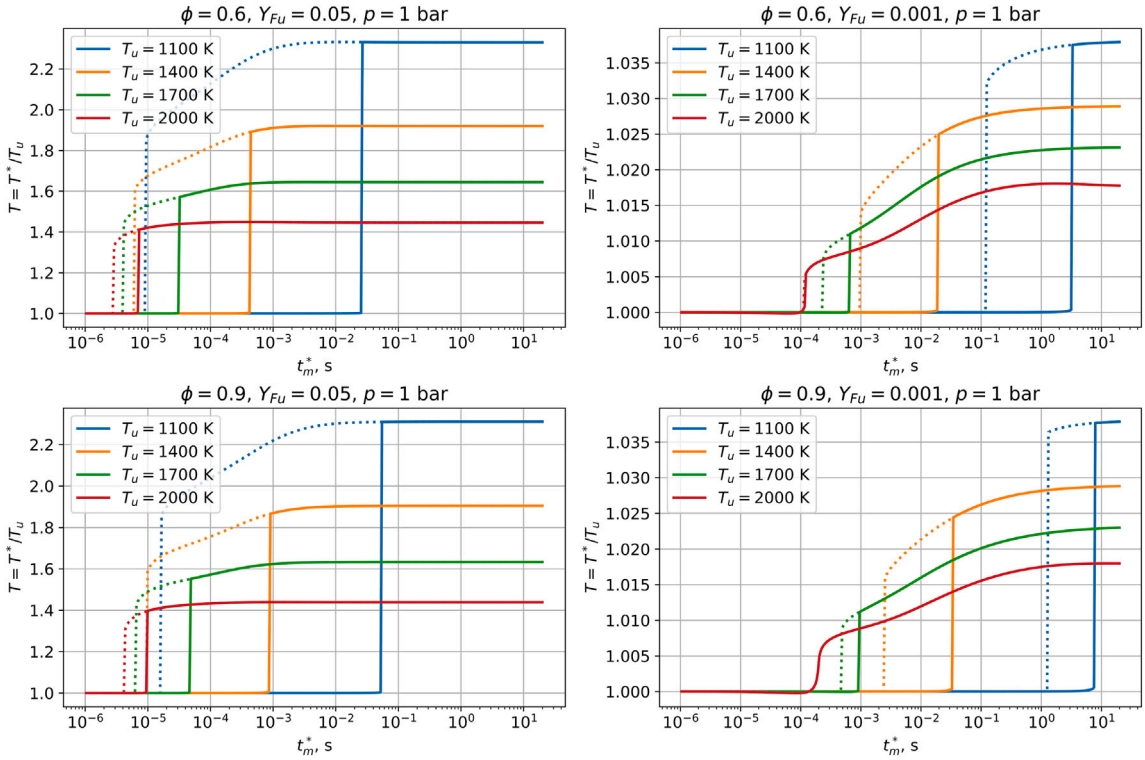

Fig. 17. The upper (dotted line) and lower (solid line) branches of the S-curves for CH_4-O_2-N_2 mixture at 4 unburned mixture temperatures, for $Y_{Fu} = 0.05$ corresponding to regular combustion and $Y_{Fu} = 0.001$ corresponding to MILD combustion, as predicted by the generalized model.

presented results were obtained for the situation in which the model discussed in this work predicts standard combustion for $Y_{Fu} = 0.05$ and MILD combustion for $Y_{Fu} = 0.001$, which correspond to the predictions presented in Fig. 14. In Fig. 17 the predicted temperatures as a function of residence times are shown, with the solid line representing the lower branch and the dotted line the upper branch. As can be observed, for large fuel mass fractions, ignition and extinction occur at significantly different residence times, as expected. For small fuel mass fractions, these points approach each other, but the S-curve becomes monotonic only for very high temperatures. The presence of chemically active radicals in the upper branch and their absence in the lower branch lead to substantial differences in system behavior, which gradually diminish as the fuel concentration decreases and the unburned temperature increases. The lack of detailed chemistry in both the model presented in this study and that of Oberlack et al. [3] results in an inability to accurately predict the system response unless these effects are properly accounted for. Nevertheless, the predicted trends, such as the effect of fuel dilution and increasing temperature resulting in a more gradual transition between unburned and burned states, are consistent with physical expectations, indicating that the models have the potential to be further refined to capture these effects more accurately. The results presented in this section are preliminary and require deeper analysis due to the applied computational method. As was shown in [8], the used approach may not lead to the same results as those obtained using steady-state solvers.

6. Conclusions

The goal of this work was to formulate governing equations and provide a numerical solution describing the generalized definition of MILD combustion for premixed flames of Oberlack et al. [3]. For this purpose, the homogeneous flow reactor model equations were used and an expression for the Damköhler number at equilibrium was found. This formula was then applied to find numerically inflection points of the $Da(T)$ curve, which define the onset of the MILD combustion regime, as previously defined by Oberlack et al. [3] for a one-step reaction. Unlike the definition of Oberlack et al., the generalized solutions provided in this study additionally include the dependence on reaction orders (α and β) and the equivalence ratio ϕ. Furthermore, unlike the previous definition, it is strictly valid from stoichiometric to lean conditions ($\phi \leq 1$). In rich conditions, the error resulting from incomplete combustion should be taken into account. This removes the limitations of the previous definition, which now incorporates various combustion conditions (stoichiometries) and reaction systems of various reactivity. Unfortunately, no analytical solution to the governing equations that define the MILD combustion boundary was found, which is due to the highly nonlinear character of the model. Instead, a numerical solution was provided in terms of graphs and approximation functions, all valid in a wide range of parameters (Q, α, β, and ϕ). If other parameter ranges are needed, the proposed numerical solution methodology can be used to find them. Two practical examples computed for hydrogen and methane were presented and discussed in detail. The influence of the parameters α, β, and ϕ on the limit curve defining the MILD combustion regime was shown to be significant, and their use will allow a more precise definition of the boundary line. Furthermore, the maximum fuel mass fractions and their corresponding oxygen mass fractions at given unburnt gas temperatures at the upper boundary of the MILD combustion were also determined. Other limitations of the method resulting from the assumptions made remain in force. It should be emphasized that the developed model is based on the assumption of premixed conditions, and its suitability for MILD combustion for non-premixed configurations, as is the case in many industrial applications, is limited. Furthermore, the role of detailed chemical kinetics appears to be essential in the prediction of combustion regimes, which could not be accurately captured by the one-step reaction and a single effective activation energy used in the current model and in [3]. These differences were highlighted by comparison with the results from the PSR model simulation, with detailed chemistry. Observed trends, however, align with the more detailed results and suggest potential for further refinement of the model to enhance its predictive accuracy. Further research can also be directed towards

finding an analytical solution or better approximation functions of the given numerical solution. The model should also be validated against experimental data.

CRediT authorship contribution statement

Adam Klimanek: Writing – review & editing, Writing – original draft, Visualization, Validation, Supervision, Software, Resources, Project administration, Methodology, Investigation, Funding acquisition, Formal analysis, Data curation, Conceptualization. **Sławomir Sładek:** Writing – original draft, Visualization, Software, Formal analysis. **Katarzyna Bizon:** Writing – review & editing, Methodology, Formal analysis, Conceptualization. **Wojciech Kostowski:** Writing – review & editing, Writing – original draft, Methodology, Data curation. **Michał T. Lewandowski:** Writing – review & editing, Writing – original draft, Methodology, Conceptualization. **Nils Erland L. Haugen:** Writing – review & editing, Methodology, Formal analysis, Conceptualization.

Declaration of competing interest

The authors declare the following financial interests/personal relationships which may be considered potential competing interests:

Adam Klimanek reports that financial support was provided by National Science Centre Poland. If there are other authors, they declare that they have no known competing financial interests or personal relationships that could have appeared to influence the work reported in this paper.

Acknowledgments

This research was funded in whole or in part by the National Science Centre, Poland, grant no. 2020/39/B/ST8/02494. This support is gratefully acknowledged. For the purpose of Open Access, the author has applied a CC-BY public copyright licence to any Author Accepted Manuscript (AAM) version arising from this submission.

Data availability

Data will be made available on request.

References

[1] Perpignan AA, Rao AG, Roekaerts DJ. Flameless combustion and its potential towards gas turbines. Prog Energy Combust Sci 2018;69:28–62. https://doi.org/10.1016/j.pecs.2018.06.002

[2] Weber R, Gupta AK, Mochida S. High temperature air combustion (HiTAC): how it all started for applications in industrial furnaces and future prospects. Appl Energy 2020;278:115551. https://doi.org/10.1016/j.apenergy.2020.115551

[3] Oberlack M, Arlitt R, Peters N. On stochastic Damköhler number variations in a homogeneous flow reactor. Combust Theor Model 2000;4(4):495–509. https://doi.org/10.1088/1364-7830/4/4/307

[4] Cavaliere A, de Joannon M. Mild combustion. Prog Energy Combust Sci 2004;30(4):329–66. https://doi.org/10.1016/j.pecs.2004.02.003

[5] Evans M, Medwell P, Wu H, Stagni A, Ihme M. Classification and lift-off height prediction of non-premixed mild and autoignitive flames. Proc Combust Inst 2017;36(3):4297–304. https://doi.org/10.1016/j.proci.2016.06.013

[6] Rao AG, Levy Y. A new combustion methodology for low emission gas turbine engines. In: Proceedings of the 8th International Symposium on High Temperature Air Combustion and Gasification, Example Conference Proceedings; Pozan, Poland: ACM Press; 2010. p. 177–85.

[7] Luan C, Xu S, Shi B, Tu Y, Liu H, Li P, et al. Re-recognition of the MILD combustion regime by initial conditions of T_{in} and X_{O2} for methane in a nonadiabatic well-stirred reactor. Energy Fuels 2020;34(2):2391–404. https://doi.org/10.1021/acs.energyfuels.9b04177

[8] Tumidajski J, Adamczyk W, Ciesielska A, Sładek S, Szlęk A, Klimanek A. Recognition of MILD combustion regimes of hydrogen oxy-combustion diluted with steam. Fuel 2025;394:135050. https://doi.org/10.1016/j.fuel.2025.135050

[9] Lewandowski MT, Pedersen KA, Løvås T. Evaluation of classical MILD combustion criteria for binary blends of ammonia, methane and hydrogen. Int J Hydrogen Energy 2024;60:566–80. https://doi.org/10.1016/j.ijhydene.2024.02.229

[10] Srinivasarao M, Sorrentino G, Reddy VM. Investigation of the interaction of the MILD regime with HiTAC and no-combustion regimes in combustion region diagrams. Front Energy Res 2024;12. https://doi.org/10.3389/fenrg.2024.1503787

[11] Ding C, Li P, Shi G, Liu Y, Wang F, Hu F, et al. Comparative study between flameless combustion and swirl flame combustion using low preheating temperature air for homogeneous fuel NO reduction. Energy Fuels 2021;35(9):8181–93. https://doi.org/10.1021/acs.energyfuels.0c04266

[12] Guo N, Lewandowski MT, Netzer C. Predictions of NOx and SOx in MILD regime based on thermal conversion of solid sewage sludge surrogates. Fuel 2023;341:127666. https://doi.org/10.1016/j.fuel.2023.127666

[13] Darabiha N, Candel S. The influence of the temperature on extinction and ignition limits of strained hydrogen-air diffusion flames. Combust Sci Technol 1992;86(1–6):67–85. https://doi.org/10.1080/00102209208947188

[14] Bray K, Champion M, Libby PA. Extinction of premixed flames in turbulent counterflowing streams with unequal enthalpies. Combust Flame 1996;107(1):53–64. https://doi.org/10.1016/0010-2180(96)00014-4

[15] Mastorakos E, Taylor A, Whitelaw J. Extinction of turbulent counterflow flames with reactants diluted by hot products. Combust Flame 1995;102(1–2):101–14. https://doi.org/10.1016/0010-2180(94)00252-N

[16] Sidey JA, Mastorakos E. Simulations of laminar non-premixed flames of methane with hot combustion products as oxidiser. Combust Flame 2016;163:1–11. https://doi.org/10.1016/j.combustflame.2015.07.034

[17] Sabia P, de Joannon M. Critical issues of chemical kinetics in MILD combustion. Front Mech Eng 2020;6. https://doi.org/10.3389/fmech.2020.00007

[18] de Joannon M, Cavaliere A, Faravelli T, Ranzi E, Sabia P, Tregrossi A. Analysis of process parameters for steady operations in methane mild combustion technology. Proc Combust Inst 2005;30(2):2605–12. https://doi.org/10.1016/j.proci.2004.08.190

[19] Sabia P, de Joannon M, Lubrano Lavadera M, Giudicianni P, Ragucci R. Autoignition delay times of propane mixtures under mild conditions at atmospheric pressure. Combust Flame 2014;161(12):3022–30. https://doi.org/10.1016/j.combustflame.2014.06.006

[20] Sorrentino G, Sabia P, Bozza P, Ragucci R, de Joannon M. Low-nox conversion of pure ammonia in a cyclonic burner under locally diluted and preheated conditions. Appl Energy 2019;254:113676. https://doi.org/10.1016/j.apenergy.2019.113676

[21] Virtanen P, Gommers R, Oliphant TE, Haberland M, Reddy T, Cournapeau D, et al. SciPy 1.0: fundamental algorithms for scientific computing in python. Nature Methods 2020;17(3):261–72. https://doi.org/10.1038/s41592-019-0686-2

[22] Moré JJ, Garbow BS, Hillstrom KE. User Guide for minpack-1 [Report ANL-80-74]. Illinois, USA: Argonne National Laboratory, Argonne; August 1980.

[23] Westbrook CK, Dryer FL. Simplified reaction mechanisms for the oxidation of hydrocarbon fuels in flames. Combust Sci Technol 1981;27(1–2):31–43. https://doi.org/10.1080/00102208108946970

[24] Kuo KK. Principles of combustion. 2nd ed. John Wiley & Sons, Inc; 2005.

[25] Turns SR. An introduction to combustion: concepts and applications, McGraw-Hill series in Mechanical engineering. McGraw-Hill; 2000.

[26] Marinov NM, Westbrook CK, Pitz WJ. Detailed and global chemical kinetics model for hydrogen. Livermore, CA (United States): Lawrence Livermore National Lab. (LLNL); 1995. https://www.osti.gov/biblio/90098

[27] Dryer F, Glassman I. High-temperature oxidation of CO and CH_4. Symp (Int) Combust 1973;14(1):987–1003. https://doi.org/10.1016/S0082-0784(73)80090-6 [Fourteenth Symposium (International) on Combustion]

[28] Yang HM, Yeo JH, Kim NI. Optimized global reaction mechanism for $H_2 + NH_3 + N_2$ mixtures. Int J Hydrogen Energy 2024;73:749–60. https://doi.org/10.1016/j.ijhydene.2024.06.102

[29] Law CK. Combustion physics. Cambridge University Press; 2006.

[30] Warnatz J, Mass U, Dibble RW. Combustion: physical and chemical fundamentals, modeling and simulation, experiments, pollutant formation. 4th ed. Berlin, Heidelberg: Springer; 2006. https://doi.org/10.1007/978-3-540-45363-5

[31] Pedregosa F, Varoquaux G, Gramfort A, Michel V, Thirion B, Grisel O, et al. Scikit-learn: machine learning in python. J Mach Learn Res 2011;12:2825–30.

[32] Sabia P, Manna MV, Ariemma GB, Sorrentino G, Ragucci R, de Joannon M. Novel insights into mild combustion processes through analyses of hysteresis behavior. Proc Combust Inst 2023;39(4):4501–7. https://doi.org/10.1016/j.proci.2022.08.011

[33] Doan N, Swaminathan N. Role of radicals on mild combustion inception. Proc Combust Inst 2019;37(4):4539–46. https://doi.org/10.1016/j.proci.2018.07.038

[34] Goodwin DG, Moffat HK, Schoegl I, Speth RL, Weber BW. Cantera: an object-oriented software toolkit for chemical kinetics, thermodynamics, and transport processes. Version 3.1.0. 2024. https://www.cantera.org. https://doi.org/10.5281/zenodo.14455267.